

See discussions, stats, and author profiles for this publication at: <https://www.researchgate.net/publication/264431350>

# Fast transmission from the dopaminergic ventral midbrain to the sensory cortex of awake primates

Article in *Brain Structure and Function* · August 2014

DOI: 10.1007/s00429-014-0855-0 · Source: PubMed

CITATIONS

5

READS

202

6 authors, including:



**Judith Mylius**

German Primate Center

12 PUBLICATIONS 58 CITATIONS

[SEE PROFILE](#)



**Max F.K. Happel**

Leibniz Institute for Neurobiology

40 PUBLICATIONS 321 CITATIONS

[SEE PROFILE](#)



**Alexander Georgievich Gorkin**

Russian Academy of Sciences

32 PUBLICATIONS 106 CITATIONS

[SEE PROFILE](#)



**Ying Huang**

Leibniz Institute for Neurobiology

51 PUBLICATIONS 232 CITATIONS

[SEE PROFILE](#)

Some of the authors of this publication are also working on these related projects:



Psychophysiology of auditory perception [View project](#)



Quantitative mapping of cytochrome oxidase and energy metabolism in the brain [View project](#)

# Fast transmission from the dopaminergic ventral midbrain to the sensory cortex of awake primates

Judith Mylius · Max F. K. Happel ·  
Alexander G. Gorkin · Ying Huang ·  
Henning Scheich · Michael Brosch

Received: 20 March 2014 / Accepted: 21 July 2014  
© Springer-Verlag Berlin Heidelberg 2014

**Abstract** Motivated by the increasing evidence that auditory cortex is under control of dopaminergic cell structures of the ventral midbrain, we studied how the ventral tegmental area and substantia nigra affect neuronal activity in auditory cortex. We electrically stimulated 567 deep brain sites in total within and in the vicinity of the two dopaminergic ventral midbrain structures and at the same time, recorded local field potentials and neuronal discharges in cortex. In experiments conducted on three awake macaque monkeys, we found that electrical stimulation of the dopaminergic ventral midbrain resulted in short-latency (~35 ms) phasic activations in all cortical layers of auditory cortex. We were also able to demonstrate similar activations in secondary somatosensory cortex and superior temporal polysensory cortex. The electrically evoked responses in these parts of sensory cortex were

similar to those previously described for prefrontal cortex. Moreover, these phasic responses could be reversibly altered by the dopamine D1-receptor antagonist SCH23390 for several tens of minutes. Thus, we speculate that the dopaminergic ventral midbrain exerts a temporally precise, phasic influence on sensory cortex using fast-acting non-dopaminergic transmitters and that their effects are modulated by dopamine on a longer timescale. Our findings suggest that some of the information carried by the neuronal discharges in the dopaminergic ventral midbrain, such as the motivational value or the motivational salience, is transmitted to auditory cortex and other parts of sensory cortex. The mesocortical pathway may thus contribute to the representation of non-auditory events in the auditory cortex and to its associative functions.

**Keywords** Deep brain stimulation · Primate · Auditory cortex · Glutamate corelease · Ventral tegmental area

---

J. Mylius (✉) · Y. Huang · M. Brosch  
Special Laboratory Primate Neurobiology, Leibniz Institute for  
Neurobiology, Brennekestraße 6, 39118 Magdeburg, Germany  
e-mail: Judith.Mylius@lin-magdeburg.de

M. F. K. Happel  
Department Systems Physiology of Learning, Leibniz Institute  
for Neurobiology, Brennekestraße 6, 39118 Magdeburg,  
Germany

A. G. Gorkin  
Institute of Psychology, Russian Academy of Sciences,  
Yaroslavskaya Street 13, 129366 Moscow, Russia

H. Scheich  
Emeritus Group Lifelong Learning, Leibniz Institute for  
Neurobiology, Brennekestraße 6, 39118 Magdeburg, Germany

H. Scheich · M. Brosch  
Center for Behavioral Brain Sciences, Otto-von-Guericke-  
University, Universitätsplatz 2, 39106 Magdeburg, Germany

## Introduction

There is converging evidence that auditory cortex is under control of dopaminergic cell structures in the ventral midbrain. Involvement of the dopaminergic ventral midbrain is suggested by the finding that neurons in auditory cortex reflect rewards given during the performance of auditory tasks and reward prediction errors (Brosch et al. 2011a). Reward-related activations are generally considered to be associated with activation of dopaminergic neurons in the ventral tegmental area and substantia nigra (Schultz 1998, 1997). In addition, auditory cortex is recruited during the performance of auditory working memory tasks (Fritz et al. 2005; Huang et al. 2012), a function generally thought to involve dopaminergic

mechanisms in the prefrontal cortex (Sawaguchi and Goldman-Rakic 1994; Chudasama and Robbins 2004). An fMRI study found that subjects had increased BOLD signals in auditory cortex in response to tones after oral application of L-dopa when they were engaged in an instrumental learning task (Weis et al. 2012). A brain slice study revealed that dopamine can modulate glutamate release in auditory cortex (Atzori et al. 2005). Dopamine could also influence auditory cortex indirectly through the inferior colliculus (Gittelman et al. 2013). Similar short-term effects of dopamine have also been demonstrated in visual cortex (Arsenault et al. 2013). In addition to these short-lasting effects, the dopaminergic ventral midbrain can also have long lasting effects on neuronal activity in auditory cortex, resulting in permanent structural changes and underlying learning (Stark and Scheich 1997; Schicknick et al. 2008, 2012; Kudoh and Shibuki 2006; Bao et al. 2001, 2003).

Dopaminergic control of auditory cortex may arise from direct and indirect inputs from the ventral tegmental area and the substantia nigra (Scheibner and Törk 1987; Campbell et al. 1987; Budinger et al. 2008), and in monkeys also from the retrorubral field (Gaspar et al. 1992; Williams and Goldman-Rakic 1998). In accordance with the rostro-caudal density gradient in cerebral cortex dopaminergic terminals and receptors show highest density in rostral regions of primate auditory cortex and their density falls off at more caudal regions (Campbell et al. 1987; Lewis et al. 1987; Lidow et al. 1991; Zilles et al. 2002; Amunts et al. 2012). At the same time, dopaminergic terminals and receptors have a layer-specific pattern in primate and human auditory cortex, with highest terminal density in layer I and in infragranular layers and highest D1-receptor density in supragranular layers (Campbell et al. 1987; Lewis et al. 1987; Lidow et al. 1991; Zilles et al. 2002; Amunts et al. 2012). Direct influences of the dopaminergic ventral midbrain on auditory cortex may also be exerted by glutamate corelease from the dopaminergic terminals (Lavin et al. 2005; Yamaguchi et al. 2011) as well as by projections of glutamatergic and GABAergic cells, which are interspersed with the dopaminergic neurons and can comprise up to 40 % of the cells in the ventral tegmental area (Margolis et al. 2006; Fields et al. 2007).

Little is known about how the projections of the dopaminergic ventral midbrain affect neuronal activity in auditory cortex (Atzori et al. 2005). Further insight into this question may be garnered from the studies in rodents that have been performed on the main target of the mesocortical pathway, namely the prefrontal cortex, and on the motor cortex. These studies have revealed that stimulation of the dopaminergic ventral midbrain or intracortical dopamine application can result in phasic ( $< \approx 1$  s) or tonic ( $> \approx 1$  s) changes of cortical neuronal activity.

Brief electrical stimulation of the ventral tegmental area and substantia nigra phasically increases or decreases neuronal activity in prefrontal cortex for up to a few hundred milliseconds. On the cellular level, initially an EPSP with a time constant of a few tens of milliseconds is evoked about 10 ms after stimulation (Bernardi et al. 1982; Mercuri et al. 1985; Lavin et al. 2005), indicating conduction velocities of the mesocortical projection system in the order of 10 m/s (Deniau et al. 1980; Thierry et al. 1980). In many neurons, the EPSP is followed by an IPSP that lasts a few hundred milliseconds. In some cortical neurons, the postsynaptic potentials result in phasic decreases and increases of their firing (Au Young et al. 1999; Ferron et al. 1984; Mantz et al. 1988; Jay et al. 1995; Pirot et al. 1992; Thierry et al. 1992). These observations in single neurons are in good agreement with the results of electrophysiological and optical recordings of cortical population activities (Lavin et al. 2005; Watanabe et al. 2009).

Pharmacological manipulations have revealed that the phasic cortical responses to electrical stimulation are not mediated by intracortical D1- and D2-receptors but rather are generated by GABA and glutamate. These transmitters are released by the mesocortical GABAergic (Carr and Sesack 2000) and glutamatergic pathway (Yamaguchi et al. 2011), or the latter coreleased from dopaminergic fibers (Lavin et al. 2005; Yamaguchi et al. 2011). The dopamine released after activation of the dopaminergic ventral midbrain still affects cerebral cortex, although in a different manner and for a longer time (Sawaguchi and Matsumura 1985; Sawaguchi et al. 1986; Matsumura et al. 1990; Jacob et al. 2013; Hosp et al. 2011; Happel et al. 2014).

In the current study, we aimed to analyze the phasic effects of activation of the dopaminergic ventral midbrain on neuronal activity in the auditory cortex of primates, i.e., in an animal model whose mesocortical dopaminergic system is more similar to that of humans than that of rodents (Berger et al. 1991; Smith et al. 2013). To this end, we adopted the paradigm that has been widely used in studying neural transmission from the dopaminergic ventral midbrain to prefrontal and motor cortex in rodents. We applied brief electrical stimulation trains to the dopaminergic ventral midbrain and measured neuronal activity in auditory cortex. With this approach, we addressed the following questions: does electrical stimulation in the dopaminergic ventral midbrain affect local field potentials (LFPs) and neuronal discharges in auditory cortex? Is the most densely expressed dopamine D1-receptor involved in these effects (Zilles et al. 2002; Amunts et al. 2012)? Are there differences between cortical layers, reflecting the layer-specific pattern of dopaminergic terminals and receptors (Campbell et al. 1987; Zilles et al. 2002; Amunts et al. 2012)? What are the auditory response properties of the neurons whose action potentials can be modified by

electrical stimulation of the dopaminergic ventral midbrain? Our experimental approach also enabled us to examine effects of dopaminergic ventral midbrain stimulation on cortex subserving other sensory modalities, i.e., the somatosensory cortex and the superior temporal polysensory cortex. The current experiments were conducted on awake animals to exclude the effects of anesthesia on the cortical state. Tonic effects of activation of the dopaminergic ventral midbrain on neuronal activity in the auditory cortex will be presented elsewhere.

## Methods

### Subjects

Experiments were conducted on three adult male Old World cynomolgus monkeys (*Macaca fascicularis*; monkeys W, I, E). They had been previously used in other studies in which they performed a behavioral task using positive reinforcement and in which neuronal activity was recorded from their auditory cortex. All experiments were carried out under approval of the animal care and ethics committee of the State of Sachsen-Anhalt (No. 28-14 42502/2-806 IfN) and in accordance with the guidelines for animal experimentation of the European Communities Council Directive (86/609/EEC).

### Animal preparation

Monkeys were surgically implanted with a head holder into the skull to allow atraumatic head fixation (Brosch and Scheich 2008). A recording chamber (21 mm diameter) was implanted over the left (monkey W and I) or the right temporal cortex (monkey E). It was centered on Horsley–Clarke coordinates A7.5 to A8.5 and D8.5 to D12.5 (conventions as in Szabo and Cowan, 1984). For all surgical procedures, monkeys were kept under deep general anesthesia with a mixture of ketamine (2 mg/kg) and xylazine (5 mg/kg). Surgery was followed by a full treatment with antibiotics (enrofloxacin, 0.2 ml/kg im) and analgesics (carprofen, 0.1 ml/kg) for up to 5 days. The dura mater was treated daily with the local disinfectant and anti-inflammatory agent Dexamytrex (Mann).

### Electrophysiology

Experiments were carried out in an electrically shielded, sound-attenuated double-walled room (1202-A, IAC) that was illuminated with an incandescent light bulb. During the experiments the head-restrained monkeys sat quietly and were awake for several hours in a primate chair. They were monitored by a video camera (ICD-848P, Ikegami) and

recorded by a computer (Pinnacle Studio 10, Pinnacle). With the aid of two separate manipulators, we inserted stimulation and recording microelectrodes through the same recording chamber into the brain (Fig. 1a).

Neuronal activity in primary auditory cortex and in adjacent parts of the overlying secondary somatosensory cortex and the underlying superior temporal polysensory

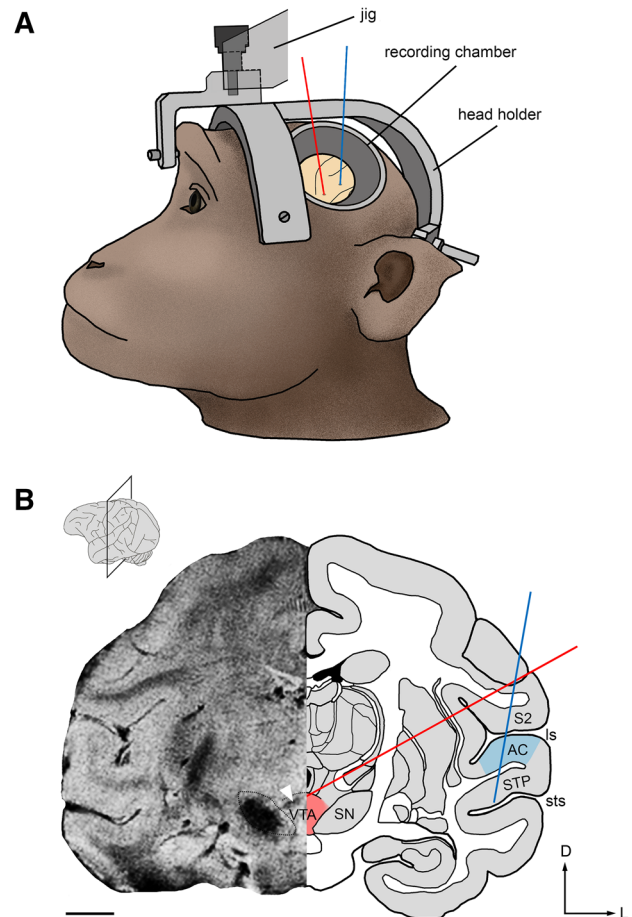


**Fig. 1** Experimental approach. **a** Schematic view of a monkey with a head holder for head restraint and a recording chamber providing access to various deep brain structures and the cortex. *Red* and *blue* lines indicate the approximate orientations of stimulation and recording electrodes, respectively. **b** Coronal section through a monkey brain at the level of the dopaminergic ventral midbrain and the auditory cortex (see inset). The left half of the section shows an anatomical magnetic resonance (MR) image of monkey I. MR contrast was optimized to highlight iron-containing brain nuclei, such as the substantia nigra (SN), indicated by the encircled region, and to highlight iron deposits. The white arrowhead points to iron deposits along an example electrode track covering the ventral tegmental area (VTA) and the contralateral SN. The right half of the section shows a corresponding anatomical schematic of cortical gray and white matter, ventricles (black), and various subcortical brain nuclei. We also highlighted other brain regions of interest for the current study, such as auditory cortex (AC), secondary somatosensory cortex (S2), superior temporal polysensory cortex (STP), lateral sulcus (ls), and superior temporal sulcus (sts). Scale bar 5 mm

cortex was recorded with a sixteen-channel microelectrode system (System Eckhorn, Thomas Recording), equipped with 5–10 tungsten microelectrodes (80  $\mu\text{m}$  diameter, 2–2.5  $\text{M}\Omega$ ). During most experiments, the electrodes were arranged in a 4-by-4 grid with a lateral spacing of 305  $\mu\text{m}$ ; sometimes electrodes were arranged as a bundle in a cannula. The electrode system was oriented slightly off the dorsoventral plane ( $10^\circ$ ). Electrodes entered the cortex between stereotactic coordinates A5 to A9 and D7.5 to D12.5 and subsequently were moved through the somatosensory cortex into the auditory cortex, and sometimes also into the superior temporal polysensory cortex (Fig. 1b). After preamplification the signal on each electrode was amplified and bandpass filtered (LFP-01, Thomas Recording; MCP-Plus, Alpha-Omega Engineering) to extract action potentials (0.5–5 kHz) and local field potentials (LFP; 0.1–100 Hz in monkey W, 1–150 Hz in monkeys I and E). All signals were fed into an AD data acquisition system (32-channel BrainWave, DataWave Technologies, 32-channel Alpha-Map, Alpha-Omega, 32-channel Cheetah, Neuralynx for monkeys W, I and E, respectively). Sampling rates for LFPs ranged between 640 and 659 Hz; for action potentials they were between 30 and 42 kHz. By means of built-in spike detection tools of the data acquisition systems (threshold crossing and spike duration), the action potentials of the somas of a few neurons in the vicinity of the electrode tip were discriminated (Supèr and Roelfsema 2005). Only the time stamps and waveforms of the action potentials were stored. From multiunit records with electrically evoked responses we extracted the spikes of single units off-line by means of principal component analysis.

### Electrical stimulation

For electrical stimulation a separate seven-channel microelectrode system was used (System Eckhorn, Thomas Recording). It was equipped with tungsten microelectrodes (80  $\mu\text{m}$  diameter) with impedances of 0.1–0.4  $\text{M}\Omega$ , which also allowed recording of neuronal activity. One of the electrodes was connected to a single-channel constant current stimulator (STG 1001, Multichannel Systems). We applied monopolar stimulation (referenced to the bolts of the implanted headholder) that consisted of short trains with six rectangular, biphasic pulses (positive first, 350  $\mu\text{s}$  phase duration, no pause) at 1,000 Hz with an amplitude of 100  $\mu\text{A}$ . These trains were repeated 50–100 times every 900 ms. During an experimental session, 50–150 of such stimulation blocks were applied to the monkeys. Our stimulations were likely strong enough to excite most cortical sites, because during occasional tests, we found robust neuronal responses already with trains consisting of

fewer pulses (3), smaller pulse frequencies (400 Hz), smaller currents (50  $\mu\text{A}$ ), and higher repetition rates (5/s).

Electrode trajectories were planned based on brain atlases (Szabo and Cowan 1984; Martin and Bowden 1996), which were refined by anatomical magnetic resonance (MR) scans of the individual monkey brains (Fig. 1b for monkey I). MR images were acquired on a 7T Scanner (Magnetom, Siemens) equipped with a head coil (Nova Medical, Inc.). Gradient echo scans (TR 266 ms, TE 15 ms, flip angle  $30^\circ$ , averages 2, FOV  $140 \times 105$  mm, matrix  $640 \times 420$ , slice thickness 1.0 mm, interslice gap 20 %) in all three planes were optimized to highlight iron-containing brain nuclei that were of interest for the current study, such as the substantia nigra and red nucleus.

Electrodes were inserted into the brain at an angle of  $28^\circ$  from the horizontal plane between stereotactic coordinates A10–A14 and D4–D7.5 and advanced up to 35 mm (Fig. 1b). In a single monkey (I) subsequent to the last recordings small iron deposits were made in the dopaminergic ventral midbrain with anodal, monophasic, direct current pulses (10  $\mu\text{A}$ , 90 s) from the tip of an iron microelectrode (80  $\mu\text{m}$  diameter, 0.3–0.6  $\text{M}\Omega$ ). After termination of experiments the head holder of monkey I was explanted, enabling MR imaging of the iron deposits to enable electrode track reconstruction (white arrowhead in Fig. 1b).

After an initial exploration phase during which we inserted electrodes at different angles into different depths of the brain, we were able to reproducibly place electrodes at the desired depths and with the desired physiological characteristics. No histological verification of stimulation sites was undertaken because in each monkey more than 100 stimulation sites were tested and all 3 monkeys of the current study are still being used for additional studies, in accordance to the principles of Replacement, Reduction, and Refinement for animal experimentation. In addition, we used the following criteria to estimate whether the electrode was within the dopaminergic ventral midbrain or within some other deep brain structure.

1. We visually and auditorily monitored the spiking activity along the entire electrode track, with a special emphasis on identifying spiking that is considered to be specific for midbrain dopaminergic cells, particularly for the substantia nigra pars compacta, such as slow tonic firing (1–10 Hz) or phasic burst firing (14–20 Hz) with characteristic bi- or triphasic action potentials of long durations greater than 2 ms (Guyenet and Aghajanian 1978; Grace and Bunney 1980, 1983, 1984a, b; Freeman et al. 1985; Freeman and Bunney 1987; Chiodo 1988; Kiyatkin 1988; Kiyatkin and Zhukov 1988; Diana et al. 1989; Grace and Onn 1989; Grace 1991).

2. Some brain structures surrounding the dopaminergic ventral midbrain can be identified by their specific physiological characteristics. Of particular help was the red nucleus which, for many of our electrode trajectories (e.g., Fig. 3a), is located immediately before the ventral tegmental area and always mediodorsal from the substantia nigra. We identified the red nucleus by (I) its specific movement-related discharges (Gibson et al. 1985), (II) its characteristic electrically evoked movements, such as movements of the contralateral proximal extremities, shoulders, and upper arms, closing of eyelids, pulling back the mouth angle, flattening the cheek, or drawing back the pinna (Delgado 1965; Larsen and Yumiya 1980; Gibson et al. 1985; Kennedy et al. 1986; Houk et al. 1988; Lovell et al. 2014), and (III) its responsiveness to acoustical stimulation (Massion and Albe-Fessard 1963; Irvine 1980; Lovell et al. 2014).
3. At selected locations, we tested whether the averaged electrically evoked field potential was modified by the dopamine D1-receptor antagonist SCH23390 (see below).
4. We evaluated the shape of the electrically evoked field potential in auditory cortex that was evoked by electrically stimulating a deep brain structure and assessed whether it matched that of the sites whose electrically evoked field potential could be modified by SCH23390.

#### Acoustical stimulation

Pure tones were generated by a computer, interfaced with an array processor (AP2-card, Tucker-Davis Technologies) at a sampling rate of 100 kHz, and D/A converted (DA1, Tucker-Davis Technologies). Tones were presented at 40 different frequencies, each repeated 10 times. Frequencies were equidistantly spaced on a logarithmic scale over a range of about eight octaves (0.11–27.2 kHz), covering the spectral sensitivity of the neurons under consideration. Tones were presented in a pseudorandom order with a constant interonset interval of 500 or 900 ms. Tone duration was 100 ms, including 5-ms ramps. In addition, we tested the neurons' auditory responsiveness with brief clicks (5 ms duration, 1-ms ramps; WG1, Tucker-Davis Technologies), which were repeated 50–150 times with a constant interonset interval of 900 ms. All signals were attenuated by a programmable attenuator (PA4, Tucker-Davis Technologies), amplified (Pioneer, A204) and coupled to a free-field loudspeaker (Manger), located approximately 1.2 m from the animal. Sounds were presented at approximately 65 dB SPL. The sound pressure level was measured with a free-field 1/2' microphone (40AC, G.R.A.S.) located near to the monkey's head.

#### Pharmacology

At selected sites, we tested whether deep brain stimulation activated the mesocortical pathway from the dopaminergic ventral midbrain to auditory cortex by either intramuscular or intracortical injections of the dopamine D1-receptor antagonist SCH23390, i.e., of the antagonist that targeted the most densely expressed dopamine receptor in primate and human auditory cortex (Zilles et al. 2002; Amunts et al. 2012). The intracortical injections served to test in one monkey (E) whether we could reproduce the effects of intramuscular injections and thus to show that SCH23390 had effects on the receptors within the auditory cortex.

For systemic applications, the monkeys received an intramuscular bolus injection of 0.03 mg/kg SCH23390 diluted in 0.1 ml/kg physiological saline in the occiput. For intracortical applications, we used different doses of SCH23390, diluted in physiological saline: 0.3  $\mu$ l of a 50 mM or 2.4–3  $\mu$ l of a 55, 62, 83, and 93 solutions. Using a Hamilton syringe, we injected these solutions over a period of 90 s via a micropipette (Thomas Recording) that was brought into the vicinity (less than 1 mm) of the recording electrodes using the same 16-channel micromanipulator that was used for the recordings from auditory cortex. Most of our intracortical injections were sufficient to affect all recording sites because a 3- $\mu$ l injection of a SCH23390 solution has been shown to spread about 3 mm into the cerebral tissue (Sawaguchi and Goldman-Rakic 1991).

To examine the time course of the effects of the antagonist on the results of deep brain stimulation, the following protocol was used. (1) We measured the preinjection activity in auditory cortex that was evoked by deep brain stimulation. (2) Within the following 5 min, the antagonist was injected. Subsequently, the electrically evoked activity was repetitively measured approximately every 5–10 min for 1–3 h, until recovery.

Control experiments included (1) electrical stimulation only without injection and (2) electrical stimulation combined with systemic injection of 0.9 % physiological saline instead of SCH23390.

#### Data analysis

Custom written MATLAB (version 2007b, MathWorks) programs were used for off-line analyses.

#### Analyses of local field potentials

##### *Evoked potentials in cortex*

For each stimulation/recording pair, we averaged the LFPs recorded in sensory cortex relative to the onset of electrical

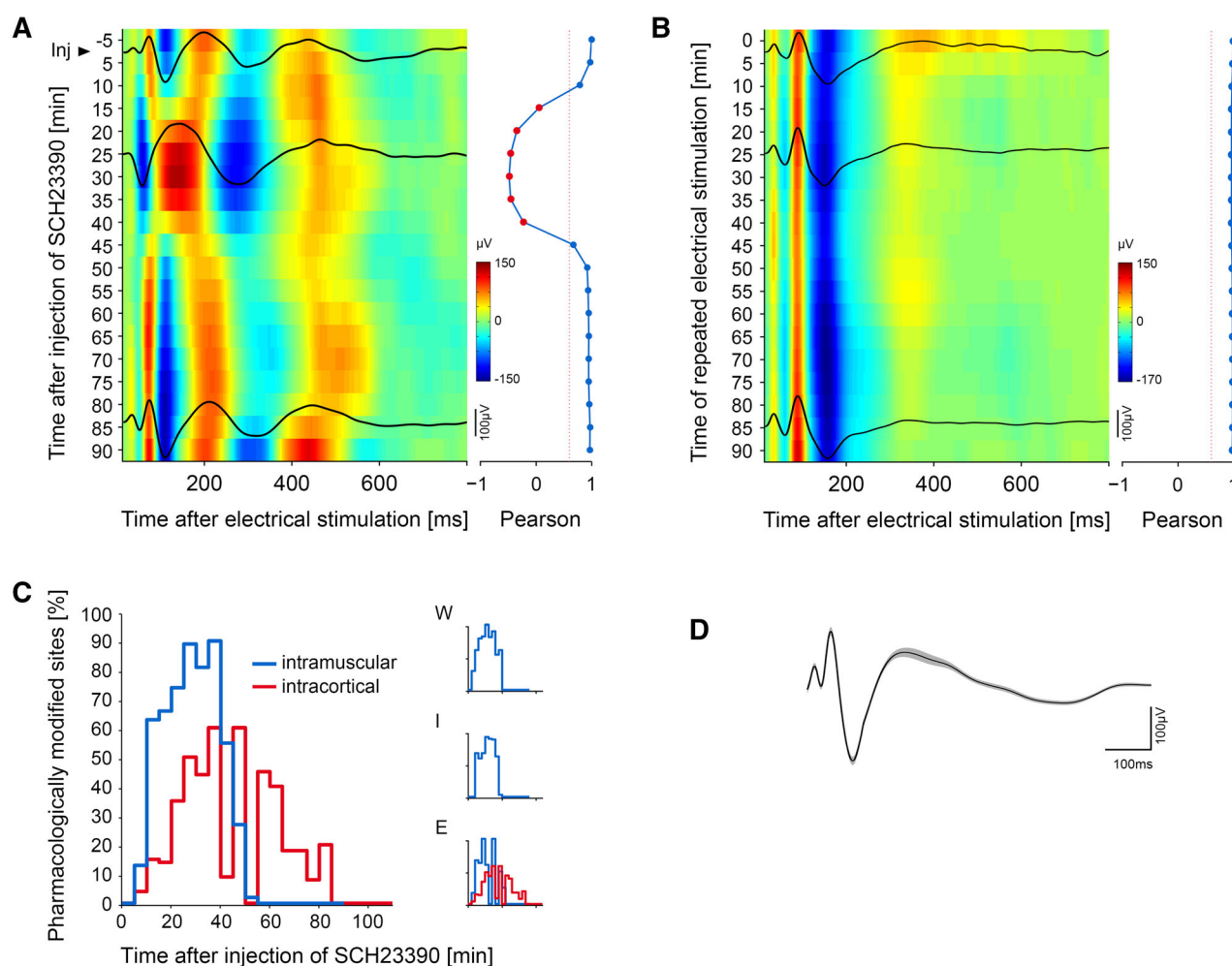


**Fig. 2** Electrical stimulation of the dopaminergic ventral midbrain evokes a polyphasic field potential in auditory cortex that is under dopamine D1-receptor control. **a** Electrically evoked potentials (EEPs) are modified after intramuscular injection of the D1-receptor antagonist SCH23390. In the heat plot, rows show color-coded amplitudes of the EEPs that were repeatedly measured after injection (red indicating positive deflections, blue indicating negative deflections). Note that from 15 to 45 min after injection EEPs were different from that before injection, whereas starting from 50 min after injection the EEP was recovered. The three black lines show the EEPs 5, 25 and 85 min after injection. The changes of the EEP were quantitatively determined by calculating the Pearson correlation between the EEP before injection with those at different times after injection (right part of a). The red dashed line denotes the correlation coefficient of 0.6 that was used to find time points at which an EEP

was modified. **b** Heat plot of the EEPs that were repeatedly measured without any pharmacological intervention (control condition). Note that the EEP was highly reproducible over the entire observation interval and that Pearson correlations were always above 0.9. **c** Time course of the effect of the D1-receptor antagonist SCH23390 on EEPs in auditory cortex. The plot shows, for different times after injection, the percentage of sites in the dopaminergic ventral midbrain from where an EEP could be elicited that was significantly modified by the antagonist. Blue and red curves indicate intramuscular and intracortical injections, respectively. Insets show data of the individual monkeys. **d** Template EEP characteristic for the dopaminergic ventral midbrain. It was obtained by averaging all EEPs that were significantly modified by the D1-receptor antagonist SCH23390 (see text). Gray shading indicates s.e.m. Note that the initial 20 ms after onset of stimulation are omitted because of the stimulus artifact

stimulation ( $\geq 50$  trials). Because the stimulation generated an artifact in the LFP records that lasted at the longest 20 ms, the initial portion of the electrically evoked potential (EEP) could not be considered in this study and, therefore, is never included in any of the EEPs shown in this article (e.g., Fig. 2a). To compensate for the default settings of the different filter systems used in the three monkeys, all EEPs were band-pass filtered between 1 and

45 Hz, using a zero-phase forward and reverse, acausal, second-order digital Butterworth filter.

For further purposes, we characterized each EEP by two measures. (1) We calculated the average root mean square (RMS) of the EEP value within the temporal interval of 20–170 ms after onset of the stimulation train. We restricted our analysis to this interval because it contained the most prominent and reproducible deflections of the

EEP. (2) We determined the similarity of an EEP to a template EEP that was characteristic of the dopaminergic ventral midbrain. To this end, we calculated the normalized cross-correlation function (mean corrected) between them and obtained its maximum (henceforth termed similarity index). The similarity index is, therefore, sensitive to the latencies of EEP excursions but not to overall EEP amplitude. Again this analysis used the interval of 20–170 ms after stimulation onset. The template EEP was calculated by averaging the EEPs that could be modified by the dopamine D1-receptor antagonist SCH23390.

For most recording sites in auditory cortex, we computed an auditory-evoked potential (AEP) by averaging all LFP traces of a recording site relative to the onset of the clicks ( $\geq 50$  trials).

#### Pharmacological modifications of local field potentials in auditory cortex

To assess effects of the D1-receptor antagonist SCH23390 on EEPs in auditory cortex, we calculated correlation coefficients (Pearson) between the preinjection EEP (i.e., the one measured before injection) and the EEPs measured at several instances in time after injection. For this analysis, again the time window of 20–170 ms after stimulation was used. Subsequently, we considered all correlation coefficients  $< 0.6$  to indicate a significantly modified EEP. This value was obtained from the control experiments in which EEPs were repeatedly measured after injection of physiological saline only or without any injection. In these control experiments, correlation coefficients were found to be rarely below 0.6 (less than 5 % of the cases).

In addition, we assessed whether the D1-receptor antagonist affected the ongoing LFP fluctuations in auditory cortex. To this end, we calculated the median of the amplitude spectrum within the delta/theta, alpha, beta, and gamma LFP frequency bands ( $< 6.7$ ,  $6.7$ – $13.4$ ,  $20.1$ – $26.9$ ,  $33.6$ – $73.9$  Hz) from the fifty 152-ms periods before each of the electrical stimulations. Subsequently, we compared the median of the amplitude spectrum within each frequency band before injection with each of those measured at different times after injection using two-sided Wilcoxon rank-sum tests ( $p < 0.05$ , Bonferroni corrected for multiple comparisons).

#### Current source density analysis and determination of cortical layers

In some experiments, we determined the laminar profile of evoked potentials in auditory cortex (EEPs and AEPs) by moving individual electrodes in steps of 100–300  $\mu\text{m}$  along tracks that were oriented almost perpendicular to the cortical surface and computed the corresponding current source density (CSD) profiles (Nicholson and Freeman

1975; Mitzdorf 1985; Steinschneider et al. 1992). The laminar profile of evoked potentials was spatially smoothed with an acausal, digital third-order low-pass Butterworth filter (spatial cutoff frequency of  $0.3 \text{ mm}^{-1}$ ). Subsequently, the second-order spatial derivative of the smoothed evoked potentials was calculated using a 5-point Hamming window as described elsewhere (Happel et al. 2010). To retain the upper and lower boundary sites, we used a linear extrapolation method, which created two additional points on each side outside of the measured range such that the second derivative of the field potential assumed no additional decay (Happel et al. 2010).

For auditory stimulation, the laminar CSD profiles of AEPs and the corresponding cascade of synaptic activations are well described (Steinschneider et al. 1992, 1998; Happel et al. 2010; Kajikawa and Schroeder 2011). Since current sources are thought to mainly reflect passive compensatory currents, we considered only the sinks for the interpretation, which for sensory stimulation were shown to indicate active depolarizing events (Mitzdorf 1985). Sinks were defined as negative components (blue colors in Fig. 5a, b) of the CSD profile if (1) they occurred in at least two contiguous CSD traces and if (2) they were  $> 2$  standard deviations below the mean baseline for at least 5 ms, computed from a 152-ms period before stimulus onset. Depending on the spatial sampling density and the extent of individual sinks usually one or two CSD traces above and below the CSD trace with the maximal amplitude of the sink were included for averaging. For each of these averaged CSD traces of an individual sink, we obtained the onset latency and the mean integral (i.e., the charge density). The onset latency of a sink was defined as the first point at which the sink was  $> 2$  standard deviations (for  $\geq 5$  ms duration) below the baseline (see Kaur et al. 2005 or Happel et al. 2010).

Cortical layers of recording sites were determined by (1) the depth relative to the cortical surface, (2) the presence and absence of (auditory-evoked) firing, (3) the shape of AEPs, and (4), if available, current sinks of auditory-evoked CSD profiles.

#### Analyses of single and multiunit activity

For each single and multiunit record in auditory cortex, we computed a post-stimulus time histogram (PSTH) with a bin size of 10 ms relative to the onset of electrical stimulation ( $\geq 50$  trials). Because electrical stimulation generated an artifact that lasted up to 20 ms (as for LFP), this period was excluded. To improve comparison between unit activities recorded at different sites, we calculated relative firing rates by dividing the PSTH through the average firing rate during the 100-ms period before the onset of stimulation.

To identify units that responded to deep brain stimulation, we compared the firing rate in the 10-ms bin immediately before stimulation with the firing rate in each of the thirty 10-ms bins post-stimulus using Wilcoxon signed-rank tests (two-sided). Firing of a site was considered to be significantly modified if at least two consecutive of the thirty bins were different from the bin immediately before stimulation at  $p < 0.0415$ , corresponding to an overall significance level of 0.05 ( $0.0415 \times 0.0415 \times 29$ ). Significant decreases were considered to reflect inhibitory responses; significant increases were considered to reflect excitatory responses. For each PSTH, we obtained the first bin with a significant difference (first-spike latency), the number of significant bins (response duration), and the firing rate and latency of the bin with the largest difference.

To assess the spectral sensitivity of a multiunit record, we analyzed its responses to the tones presented at 40 different frequencies and obtained the best frequency, and first-spike latency as described elsewhere (see Brosch et al. 1999).

#### Pharmacological modifications of multiunit activity

To uncover effects of the D1-receptor antagonist on multiunit activity in auditory cortex, we compared the PSTH that was measured before drug injection with the PSTHs that were measured at different times after injection. To identify effects on electrically evoked multiunit responses, we tested each PSTH for the presence or absence of such responses. A multiunit was then considered to be affected by the antagonist if an electrical response temporarily disappeared after drug injection or if an electrical response temporarily emerged at a previously unresponsive site. To identify effects on the spontaneous firing, we analyzed whether the spontaneous firing changed after injection of the D1-receptor antagonist by means of Wilcoxon rank-sum tests (two-sided,  $p < 0.05$ , Bonferroni corrected for multiple comparisons). The spontaneous firing was obtained from the 100-ms period before electrical stimulation.

## Results

In total, we tested at 567 deep brain sites in three monkeys (238, 157 and 172 in monkeys W, I, and E, respectively) how electrical stimulation affected neuronal activity at 2,607 recording sites (1,202, 491, and 914 in monkeys W, I, and E, respectively) in the primary auditory cortex, in the secondary somatosensory cortex and in the superior temporal polysensory cortex. The data were from 114 experimental sessions in which we accessed the dopaminergic ventral midbrain and surrounding deep brain structures by

moving stimulation electrodes along approximately dorsoventrally oriented paths and in which we recorded LFPs and neuronal discharges preferentially from the granular layers of primary auditory cortex.

#### Influence of the dopaminergic ventral midbrain on local field potentials in sensory cortex

The upper black line in Fig. 2a shows that brief monopolar electrical stimulation of the dopaminergic ventral midbrain evoked a polyphasic potential in auditory cortex that consisted of several separable positive and negative deflections. In this experiment, electrode placement was based on stereotactic coordinates, anatomical MRI measurements, and a physiological landmark (i.e., the red nucleus). We obtained additional evidence that the electrical stimulation excited the dopaminergic ventral midbrain (i.e., the ventral tegmental area or the substantia nigra) by finding that the EEP could be modified by the D1-receptor antagonist SCH23390. This is illustrated in Fig. 2a, which shows color-coded EEPs that were repeatedly measured after injection of the antagonist. We noted that from about 15–40 min after injection, a differently shaped EEP was observed. After even longer periods EEPs were again similar to that obtained before injection; thus the original EEP was recovered. Note that at all times after injection an EEP of some shape could be elicited, suggesting that the dopamine antagonist only modulated neural transmission from the dopaminergic ventral midbrain to auditory cortex, but did not completely block it.

To quantitatively assess how long the dopamine antagonist affected the EEP, we calculated correlation coefficients (Pearson) to measure the relationship between the EEP measured before injection with those measured after injection (Fig. 2a, right panel). This analysis revealed that correlation coefficients remained at high levels until 10 min after injection, and then markedly decreased and, at some time, even attained negative values; the latter indicates substantial anticorrelation and, thus, partially opposite phase relationships between the EEPs obtained before and after injection. After being most negative 30 min after injection, the correlation coefficient increased again and then remained at high levels from about 45 min after injection.

To determine which changes of correlation coefficients indicated a statistically significant effect of the antagonist on the EEP, we assessed the variance of such EEPs when they were repeatedly measured without any pharmacological intervention. As shown for another stimulation/recording pair (Fig. 2b), we found that in this condition the EEP was highly reproducible over a period of 90 min. This was also seen for another 18 sites that were estimated to be located in the dopaminergic ventral midbrain and that had

similar EEPs. The high stability of EEPs was reflected in generally high correlation coefficients that were only rarely (<5 % of all cases) below 0.6. Thus, we considered decreases of correlation coefficients below this critical value to indicate a statistically significant change of an EEP. In the example shown in Fig. 2a, we therefore concluded that the dopamine antagonist affected the EEP from 15 to 40 min after injection.

#### Population analysis of electrically evoked potentials in auditory cortex

At 44 of the deep brain sites (including the one shown in Fig. 2a), we determined whether dopamine was involved in the transmission of neuronal signals to the auditory cortex by injecting the D1-receptor antagonist SCH23390. For 28 (63.6 %) of these sites, we found that SCH23390 significantly modified the EEP recorded in auditory cortex (i.e., at least one of the correlation coefficients computed from the preinjection EEP and the postinjection EEP was below the critical value of 0.6), with no large difference between injections made intramuscularly (21/31) and into auditory cortex (7/13). This was found at 135 of 212 sites (63.7 %) in auditory cortex. Modifications occurred between 5 and 85 min after injection and were most prevalent 25–40 min after injection (Fig. 2c). Notably, EEP changes were exclusively observed when deep brain sites were located in the dopaminergic ventral midbrain (28/41). By contrast, no such changes were observed for EEPs obtained from sites >4 mm dorsally from the dopaminergic ventral midbrain (0/3), which also had very different EEP shapes (e.g., see Fig. 3a). This suggests that the shape of the EEP elicited from the dopaminergic ventral midbrain is distinct from the shapes of EEPs that were elicited from locations outside this deep brain structure. This observation was, therefore, used as an additional means to determine whether a deep brain site that was not pharmacologically tested was inside or outside the dopaminergic ventral midbrain, namely to electrically stimulate this site and determine whether the resulting EEP was similar to the EEP that is specific for the dopaminergic ventral midbrain. To assess this similarity, we calculated the normalized cross-correlation function between an EEP and a template EEP that is specific for the dopaminergic ventral midbrain. The template EEP is the average of the 28 EEPs that were modified by the D1-receptor antagonist SCH23390, and consists of several positive and negative deflections with amplitudes of  $-175$  to  $130 \mu\text{A}$  within a time range of about 400 ms (Fig. 2d). Because its most prominent and reproducible deflections were in the time window of 20–170 ms after stimulation only this time window was used for the calculation of the cross-correlation function. For further purposes, we obtained the maximum from the cross-correlation function

and considered all EEPs to match the template EEP if this similarity index exceeded 0.8.

The observed changes of EEPs after injection of SCH23390 are compatible with the interpretation that the EEP results from a superposition of postsynaptic potentials (Jervis et al. 1983) that is modified by the D1-receptors. The alternative view of EEP generation is that the volley of action potentials arriving after electrical stimulation resets the phase of spontaneous cortical oscillations so that activity at particular frequencies becomes phase locked (Sayers et al. 1974). This view is not compatible with the effects of SCH23390 on spontaneous LFP oscillations. Specifically, we tested whether LFP amplitudes in the delta/theta, alpha, beta, and gamma frequency bands (<6.7, 6.7–13.4, 20.1–26.9, 33.6–73.9 Hz) changed after injection of SCH23390. The spontaneous LFP fluctuations were obtained from the 152-ms periods before the onsets of electrical stimulation trains. Although there were significant (Wilcoxon rank-sum tests, two-sided,  $p < 0.05$ ) changes found for individual deep brain sites the incidence of these changes was not above the chance level obtained in our control experiments.

#### Characterization of electrically evoked potentials elicited from dopaminergic ventral midbrain and adjacent deep brain sites

Figure 3a shows examples of the different EEP shapes measured in granular layer of auditory cortex that were elicited from different deep brain sites by moving a stimulation electrode along an approximately ventromedially oriented path into the ventral tegmental area. In this track, the red nucleus could be unequivocally identified because electrical stimulation evoked body movements that are specific for this nucleus (Lovell et al. 2014). After failing to evoke these body movements, we concluded that the electrode had reached the ventral tegmental area. We noted that from every site along the entire track an EEP could be elicited. Their shapes and amplitudes, however, varied considerably. For the current study, it is of interest that the EEPs elicited within the range from 23.5 to 29.75 mm below cortical surface were all highly similar to each other and had similar amplitudes. This range corresponds to the location of the ventral tegmental area. That EEPs within this range were elicited from the ventral tegmental area was further indicated by finding that all EEPs had high similarity indices (>0.8), i.e., they were highly similar to the template EEP, which is specific for the dopaminergic ventral midbrain (see above). By contrast, EEPs elicited from outside this range (e.g., the red nucleus) had small similarity indices (<0.5) and larger amplitudes.

From 381 of the 523 deep brain sites (72.9 %) that were not pharmacologically tested, we elicited EEPs at 1,748 of

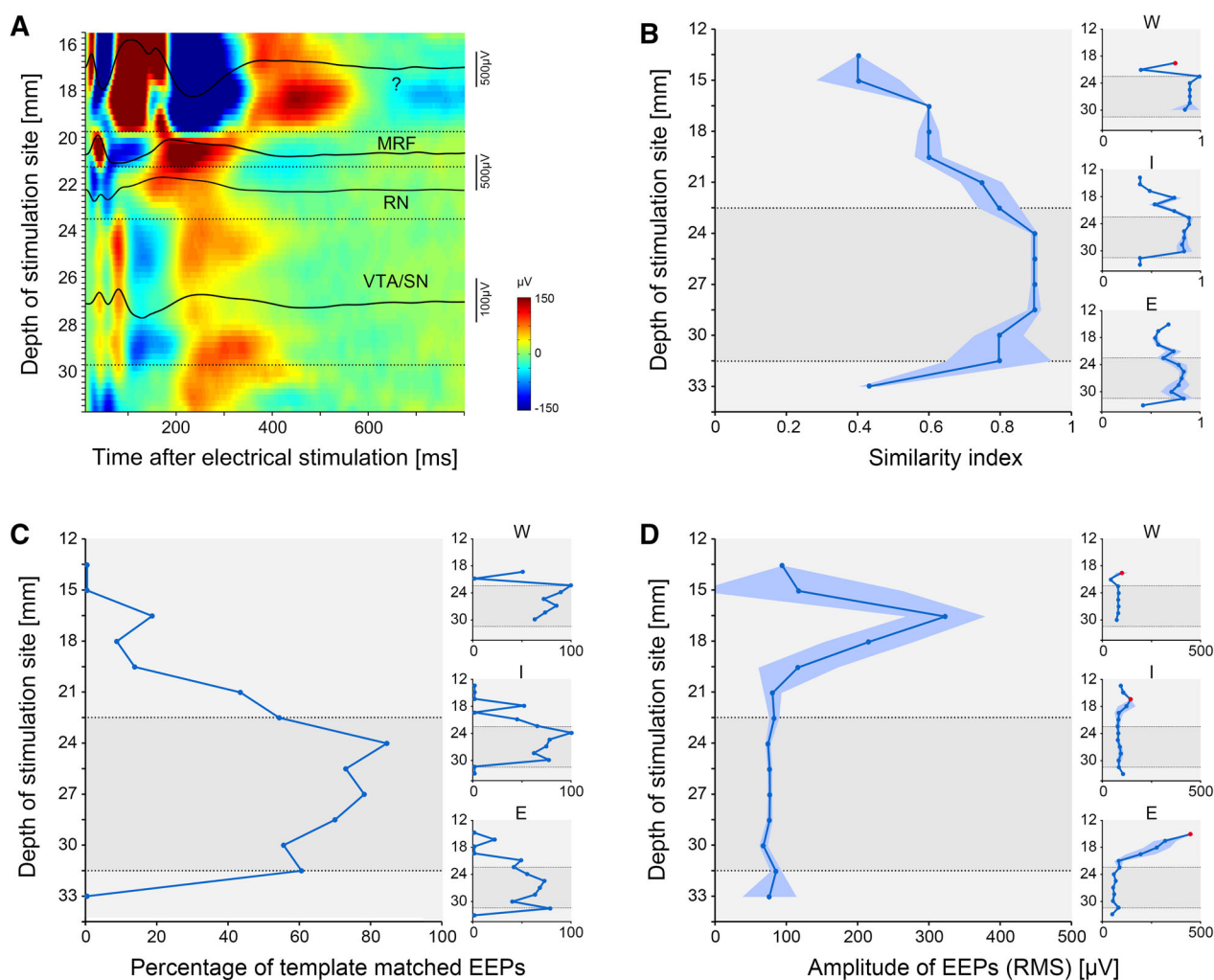


**Fig. 3** EEPs elicited from the dopaminergic ventral midbrain differ from those elicited from other deep brain sites. **a** Examples of the EEPs that were elicited from different deep brain sites by moving a stimulation electrode along a track that was oriented at an angle of  $28^\circ$  from the horizontal plane. Depth was measured relative to cortical surface. In the heat plot, each row shows the color-coded amplitudes of the EEP that was elicited from the depth given on the ordinate. Amplitudes above and below  $150 \mu\text{V}$  were clipped. The four black lines show the EEPs from selected deep brain sites, such as the dopaminergic ventral midbrain, i.e., the ventral tegmental area (VTA) and the substantia nigra (SN), the red nucleus (RN), the midbrain reticular formation (MRF) and unidentified sites, separated by horizontal dotted lines. Note that EEPs elicited from within the dopaminergic ventral midbrain (VTA/SN) were highly similar to each other but different from those elicited from outside the VTA/SN. For

2,395 (73.0 %) recording sites in auditory cortex with a significant similarity index ( $>0.8$ ), i.e., the EEPs that could be elicited from them matched very well the EEP of the sites where the D1-receptor antagonist could modify the EEP. Sites with a significant similarity index were preferentially located within a range of  $\sim 9$  mm centered around 27 mm below cortical surface. Within this range  $>50$  % of the EEPs had a similarity index  $>0.8$  (Fig. 3c), and the

illustrative purposes, the depth profiles of two adjacent electrode tracks were pooled and smoothed with a spatial constant of  $400 \mu\text{m}$ . The electrode track corresponds to a track similar to the one shown in Fig. 1b. **b–c** Variation of median similarity index of EEPs (**b**) and the percentage of EEPs that were similar to the template EEP (**c**) with depths of the stimulation sites for all monkeys (main panel) and for individual monkeys (insets). The similarity index is defined as the maximum of the cross-correlation function between an individual EEP and the template EEP (see Fig. 2d). An EEP was considered to be similar to the template EEP if the similarity index was  $\geq 0.8$ . **d** Variation of the median amplitudes (root mean square) of EEPs with depth of the stimulation site. Root mean squares were calculated from the time range of 20–170 ms after stimulation onset. Insets indicate results of the three monkeys individually

median similarity index was  $>0.8$  (Fig. 3b). These spatial measures are in good correspondence with the location of the ventral tegmental area and the substantia nigra based on physiological landmarks and published brain atlases (Szabo and Cowan 1984; Martin and Bowden 1996). Within the range of high similarity indices, EEP amplitudes were relatively constant (expressed as median RMS values in the time range of 20–170 ms after stimulation onset, Fig. 3d).

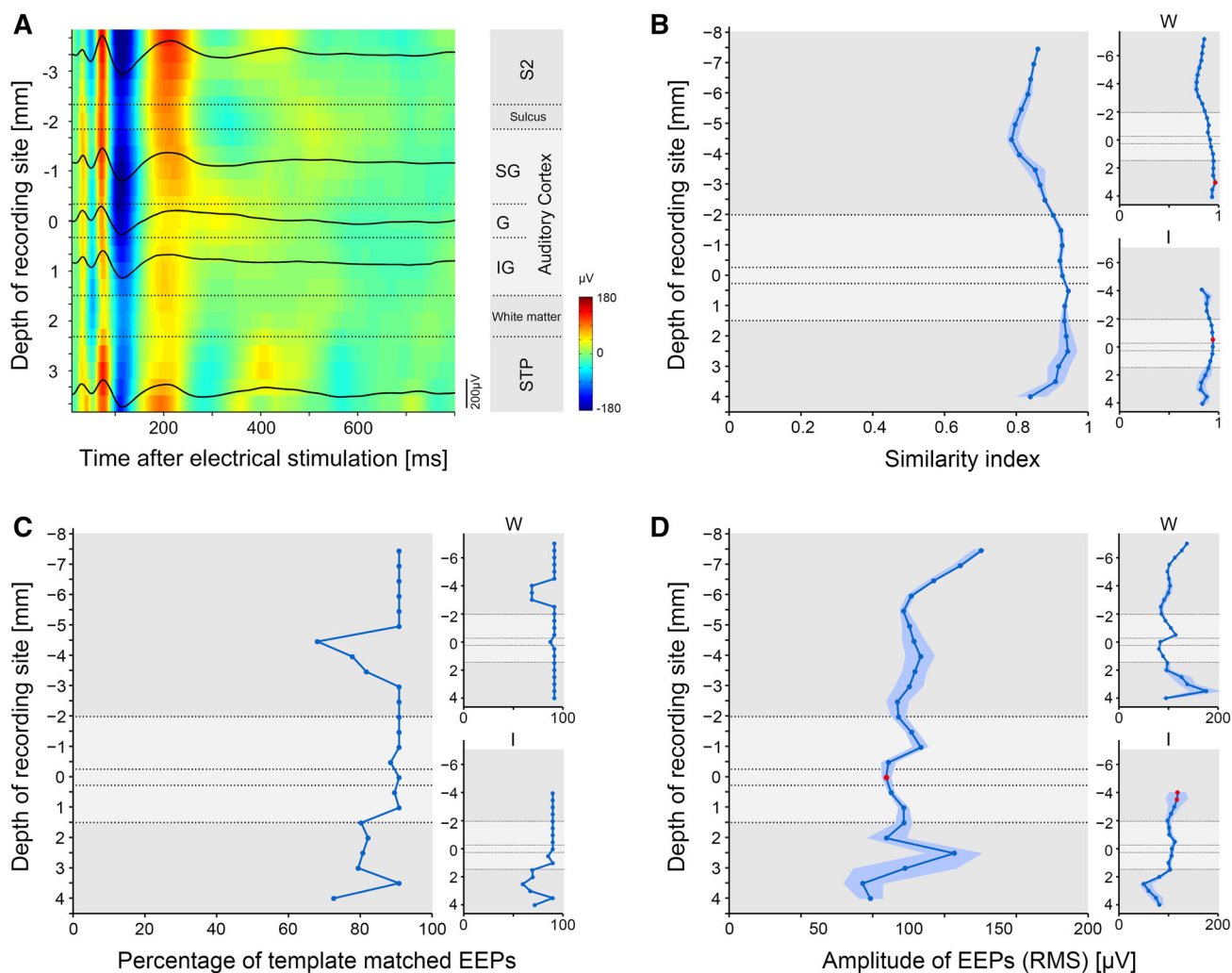


**Fig. 4** Highly similar EEPs in different layers of the auditory cortex and in the somatosensory cortex and the superior temporal polysensory cortex. **a** Examples of the EEPs that were elicited at different sites of the auditory cortex, the somatosensory cortex and the superior temporal polysensory cortex by stimulating a location in the dopaminergic ventral midbrain. The cortical recordings were obtained by moving an electrode along a trajectory that was oriented slightly off the dorsoventral plane ( $10^\circ$ ). Depth is given relative to the granular layer of auditory cortex. In the heat plot, each row shows the color-coded amplitudes of the EEP that was measured at the depth given on the ordinate. Amplitudes above and below  $180 \mu\text{V}$  were clipped. The five black lines show the EEPs at selected depths. Approximate locations of the secondary somatosensory cortex (S2), the lateral sulcus (ls), the supragranular (SG), granular (G), and

infragranular (IG) layer of auditory cortex, the white matter, and the superior temporal polysensory cortex (STP) are indicated right of the heat plot. **b–c** Variation of median similarity index of EEPs (**b**) and the percentage of EEPs that were similar to the template EEP (**c**) with depths of the recording sites for all monkeys and for individual monkeys (*insets*). The similarity index is defined as the maximum of the cross-correlation function between an individual EEP and the template EEP (see Fig. 2d). An EEP was considered to be similar to the template EEP if the similarity index was  $\geq 0.8$ . **d** Variation of median amplitudes (root mean square) of EEPs with depth of recording site. Root mean squares were calculated from the time range of 20–170 ms after stimulation onset. *Insets* show the two monkeys individually. Red dots indicate statistically significant measures (see “Methods”)

Electrically evoked potentials in different layers of auditory cortex and in the somatosensory cortex and the superior temporal polysensory cortex

For 17 sites in the dopaminergic ventral midbrain, we tested how electrical stimulation affected LFPs in auditory cortical layers other than the granular one and in other sensory cortices. To this end, we placed stimulation

electrodes at fixed positions in the dopaminergic ventral midbrain and measured EEPs at different depths of the auditory cortex, the somatosensory cortex and the superior temporal polysensory cortex by moving recording electrodes along 63 trajectories that were oriented approximately perpendicular to the surface of auditory cortex.

Examples of the EEPs that were measured along such an electrode track are given in Fig. 4a. We noticed that, within

the investigated time window of 20–170 ms post-stimulus, the major excursions of the EEPs were very similar at all depths and thus in all cortical layers of auditory cortex. At later times, EEP excursions were more variable. In addition, we noticed that major excursions of the EEPs were very similar in the auditory, somatosensory, and superior temporal polysensory cortex. These observations were quantitatively confirmed by finding that all EEPs in this track had high similarity indices ( $>0.8$ ).

For the remaining 16 sites in the dopaminergic ventral midbrain, we confirmed that EEPs were highly similar at different depths of the auditory and the somatosensory cortex as well as of the superior temporal polysensory cortex. Neither the similarity index of the EEPs (Fig. 4b) nor the percentage of EEPs with high similarity to the template EEP (Fig. 4c) varied significantly with cortical depth [bootstrap,  $p > 0.05$ . For the bootstrap procedure, we iteratively (100,000 times) obtained from all 17 stimulation sites the variation of the random depth profile for the similarity index (or the number of template matched EEPs) by randomly shuffling with replacement the cortical depth/similarity index pairs of a stimulation site]. Despite considerable variation across individual tracks, the amplitudes of the EEPs were generally quite similar at different sites of the auditory and the somatosensory cortex as well as of the superior temporal polysensory cortex. Although our bootstrap analysis was not able to reject such a dependence ( $p < 0.05$ ), a significant difference was present at a single cortical depth only, which according to additional analyses (see below), corresponded to the supragranular layer of auditory cortex (Fig. 4d).

#### Laminar current source density profiles of electrically evoked potentials in auditory cortex

Although EEP excursions appeared at similar latencies at different depths of auditory cortex, when the interval from 20 to 170 ms after stimulation was considered, amplitudes of individual excursions were quite variable. This is exemplified in Fig. 5a in which EEPs were sampled with a higher spatial density than in Fig. 4a. The variability of EEP amplitudes is best visible in the color-coded representation of the EEPs, which demonstrates that some of the later EEP peaks after 170 ms, even changed polarity with cortical depth, particularly the one around 220 ms. To better assess the layer-specific activation of auditory cortex, we, therefore, performed a CSD analysis on the EEPs that were measured at different cortical depths. To tune up our method and to have a better estimate of the cortical layer from which LFPs were recorded, we also performed a CSD analysis on click-evoked potentials.

The auditory-evoked CSD profiles were similar to those obtained with click and tone stimulation in previous studies

on the auditory cortex of monkeys (Steinschneider et al. 1992, 1998; Kajikawa and Schroeder 2011) and rodents (Happel et al. 2010, 2014). Earliest click-evoked current sink activation was found in the ventral most recordings from auditory cortex, i.e., in deeper layers, with a median onset latency of 28.0 ms (interquartile range, IQR = 1.7 ms) after stimulation. This was followed by a sink (60.0 ms, IQR = 0.2 ms) in the middle portions of auditory cortex. Subsequent sink activations were found again in deeper layers around 126 ms (IQR = 6.6 ms) and in upper parts (200 ms, IQR = 2.1 ms). The last sink in upper parts was usually the most prominent one, i.e., the one with the greatest charge density. This spatiotemporal cascade of sinks was found in 34 of 35 CSD profiles which we obtained during 8 experimental sessions in three monkeys (Fig. 5c, dark gray bars). Based on the similarity of our findings with those obtained in the cited earlier studies, we assigned recordings with early and late sinks in the ventral most parts of auditory cortex to infragranular layers, recordings with a sink in the middle parts of auditory cortex to granular layers, and recordings with a sink in the dorsal most parts of auditory cortex to supragranular layers.

For the interpretation of laminar EEP profiles, we used the same reasoning that has been established for laminar AEP profiles, namely that only current sinks indicate synaptic activations and should therefore be described (Müller-Preuss and Mitzdorf 1984; Mitzdorf 1985; Steinschneider et al. 1992; Happel et al. 2010). The representative example in Fig. 5a shows that electrical stimulation in the dopaminergic ventral midbrain evoked a highly specific cascade of current sinks across cortical layers. The same cascade of four sinks was present in almost all CSD profiles (59 of 63), which we obtained during 17 experimental sessions in two monkeys. The cascade of current sinks usually started with an early infragranular sink at 42 ms (IQR = 3.0 ms), which was followed by a granular sink at 95 ms (IQR = 1.7 ms), by another late infragranular sink at 132.5 ms (IQR = 5.7 ms), and a supragranular sink at 235.5 ms (IQR = 12.3 ms) (Fig. 5c, light gray bars). Compared to the timing relationships of the sinks, there was more variation of the strengths of the different sinks among the 63 electrically evoked CSD profiles (Fig. 5d). The largest sinks (expressed as the charge density, i.e., the integral of the current flow during the presence of a sink) were the late infragranular and the supragranular sinks, and the weakest sink was the early infragranular sink (Fig. 5d, light gray bars).

Interestingly, the same spatiotemporal cascade of sinks was observed when auditory instead of electrical stimuli were tested, that is, an early infragranular sink was followed by a granular sink, a late infragranular sink and a supragranular sink (Fig. 5b). We noticed that for the

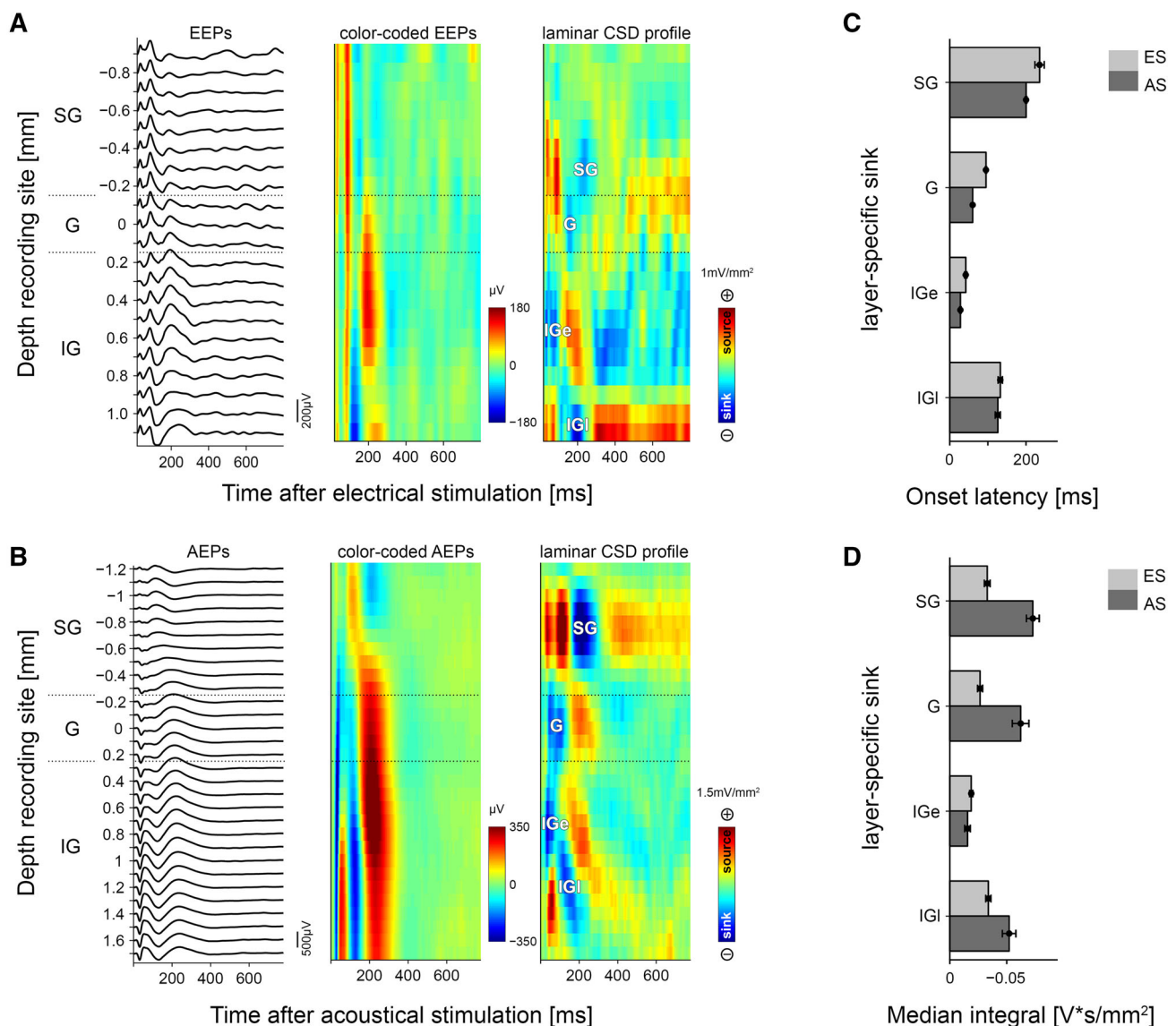


**Fig. 5** Electrically and acoustically evoked potentials in different layers of auditory cortex and corresponding current source density profiles. **a** Representations of EEPs recorded at different depths of auditory cortex by lines (left panel) and by a heat plot (middle panel) as well as corresponding second spatial derivatives of EEPs (CSD profile; right panel). Note the layer-specific activation sequence of current sinks (blue colors), starting in upper parts of the infragranular layer (IGe), followed by those in granular layers (G), deeper parts

stimulation parameters used in the present study auditory sinks were consistently earlier and had larger amplitudes than electrical sinks. It is not clear whether these relationships change if different auditory or electrical stimuli would be tested. The similarities in the temporal order of the intracolumnar signal flow was unlike the strengths of synaptic activations evoked by auditory and electrical stimulation, which was strongest in supragranular layers, followed by that of granular layers and weakest for the early infragranular sink (Fig. 5d, dark gray bars).

the infragranular layers (IGI) and in supragranular layers (SG). **b** Depth profile of AEPs and corresponding CSD profile. Note that the activation sequence of current sinks was similar to that for the EEP shown in **a** and that the range of recording depths is greater than in **a**. **c** Median and interquartile range (IQR) onset latencies of the four sinks obtained from the CSD profiles for electrical (ES; light gray bars) and acoustical (AS; dark gray bars) stimulation. **d** Median and IQR charge densities of the four sinks obtained from the CSD profiles

#### Influence of the dopaminergic ventral midbrain on neuronal firing in auditory cortex

Electrical stimulation of the dopaminergic ventral midbrain could also affect neuronal firing in auditory cortex. This was found when we analyzed 235 sites in this deep brain structure. They were from the 409 sites from which an EEP could be elicited that was highly similar to the template EEP (similarity index  $>0.8$ ; the remaining 174 sites were excluded for technical reasons). For each of the 235 deep

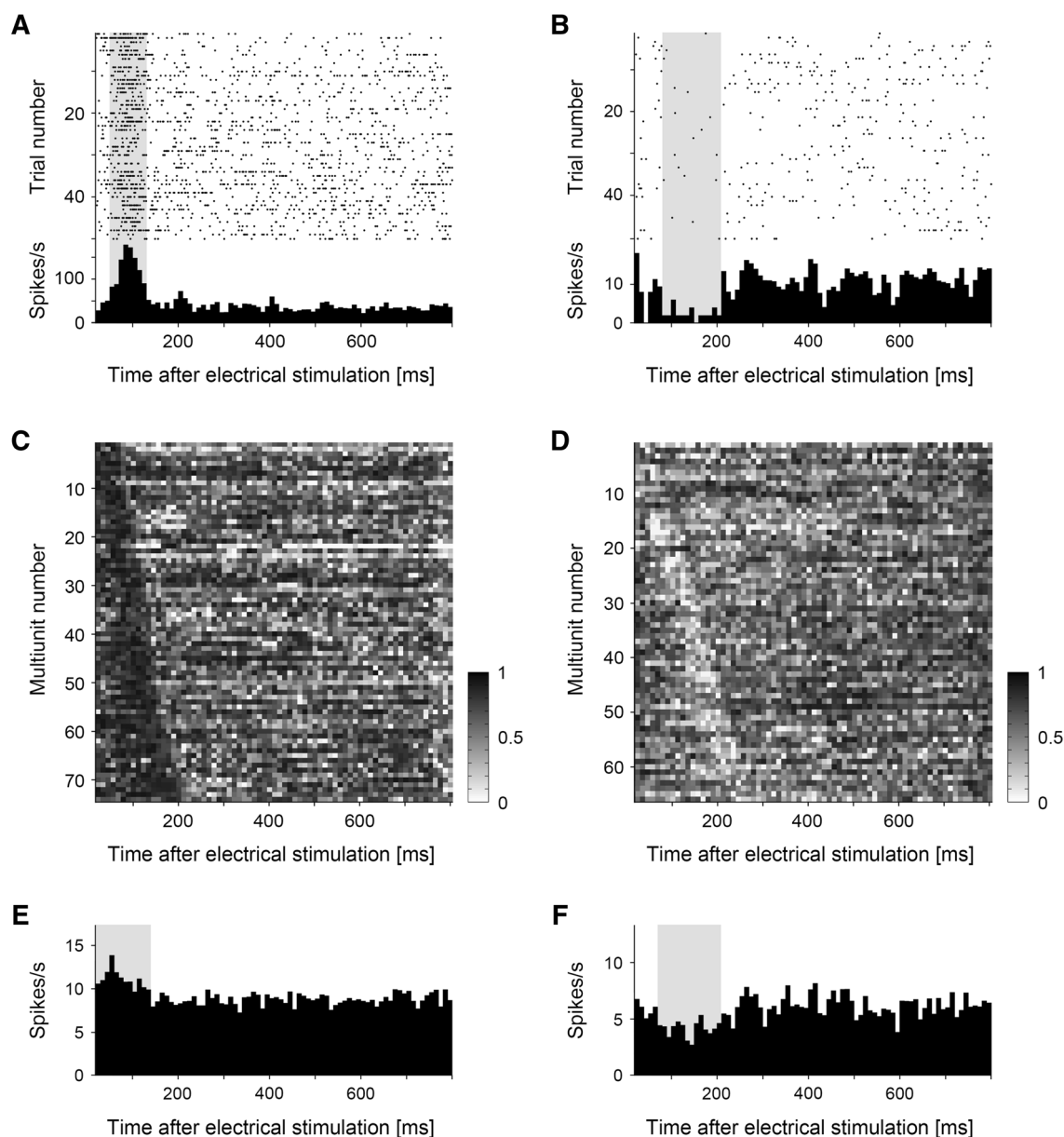


**Fig. 6** Single and multiunit responses in auditory cortex evoked by electrical stimulation of the dopaminergic ventral midbrain. **a** Representative multiunit recording with an excitatory response. In the raster display, each *dot* in a horizontal raster line indicates the occurrence of a spike relative to onset of electrical stimulation. Different raster lines refer to the 50 repetitions of electrical stimulation. The *lower panel* shows the average firing rate (PSTH) relative to the onset of electrical stimulation. The *gray-shaded area* indicates the time interval during which the firing rate was significantly different from the firing rate in

the 10-ms bin immediately before stimulation onset (Wilcoxon signed-rank test, two-sided). **b** Representative multiunit recording with an inhibitory response. **c** *Gray-coded* plot of the 74 multiunits with excitatory electrical responses. Each *row* shows the time course of the relative firing rate of an individual multiunit encoded on a *grayscale*. **d** *Gray-coded* plot of the 66 multiunits with inhibitory electrical responses. **e–f** Population PSTH of the 42 single units with excitatory responses (**e**) and the 15 single units with inhibitory (**f**) responses

brain sites, we analyzed the effects of stimulation on up to seven sites in auditory cortex. The number of cortical sites was variable because only multiunit recordings were considered at which the neurons responded to tones or clicks (755) and/or responded to electrical stimulation (140, see below), such that a total of 769 multiunit recordings in auditory cortex entered our analyses.

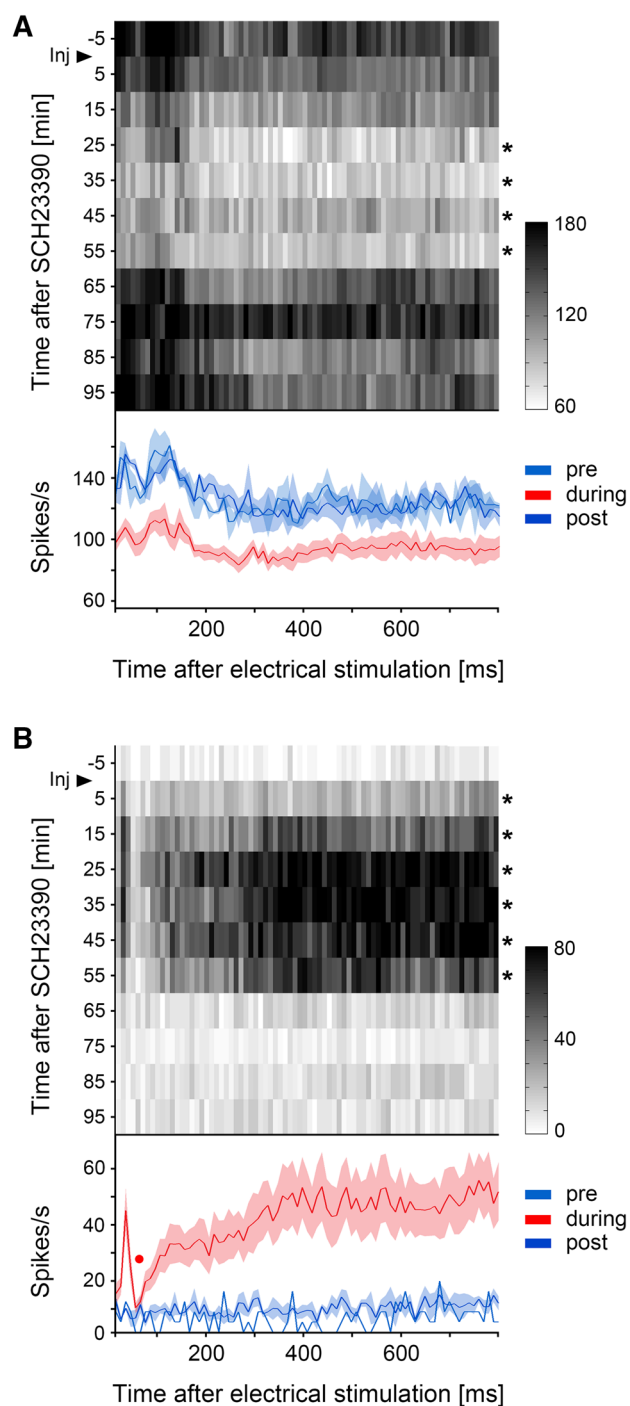
Figure 6 shows two example sites in auditory cortex where the multiunit activity was briefly increased (panel A) or decreased (panel B) for tens of milliseconds shortly after electrical stimulation of the dopaminergic ventral midbrain. Such phasic responses were seen at 140 of the 769 sites in auditory cortex (18.2 %) and could be elicited from 89 of 235 (38 %) sites in the dopaminergic ventral

**Fig. 7** Temporary modification of electrically evoked multiunit responses in auditory cortex by blocking the dopamine D1-receptor. **a** Temporary suppression of the excitatory electrical response. Each row in the upper panel shows the time course of the firing rate in response to electrical stimulation (on a gray scale) before and at several points in time after injection of the D1-receptor antagonist SCH23390. Note the overall decrease of firing and the loss of the excitatory electrical response from 25 to 55 min after injection. Stars indicate significant changes of the evoked firing. The lower panel shows the average firing rate (PSTH) of this multiunit relative to the onset of electrical stimulation before injection (light blue curve), 25–55 min after injection (red curve), and from 65 min after injection (dark blue). **b** Temporary emergence of an inhibitory electrical response at ~62 ms (red dot). Note the overall increase of firing and the emergence of the inhibitory electrical response from 5 to 55 min after injection. Also, note that the initial peak at ~37 ms, superimposed on the inhibitory response, does not exceed the baseline firing rate and is, therefore, not considered an excitatory response in this multiunit recording

midbrain. Unlike all EEPs, electrical multiunit responses were (with 1 exception) always monophasic. About half of the responses ( $n = 74$ , 52.9 %) were excitatory. The remaining 66 responses (47.1 %) were inhibitory ones. The characteristics of all electrical multiunit responses are shown in panels C and D of Fig. 6, respectively. Generally, excitatory responses occurred significantly earlier than inhibitory responses after stimulation (Wilcoxon rank-sum tests, two-tailed,  $p < 0.0034$ ). Median first-spike latencies of excitatory responses were 35.0 ms (IQR = 4.3 ms), those of inhibitory responses 50.0 ms (IQR = 8.0 ms). The median time of maximal excitation was 75 ms (IQR = 7.6 ms) and that of maximal inhibition was 130 ms (IQR = 14.9 ms). At these times, excitatory responses were increased to 160 % (IQR = 10 %) above the spontaneous firing; inhibitory responses were reduced to 50 % (IQR = 3 %) of the spontaneous firing. Median duration of both types of electrical responses were equal (60.0 ms; IQR = 4.3 ms and IQR = 5.7 ms, respectively, Wilcoxon  $p > 0.05$ ).

The sites with electrical responses had auditory response properties that did not differ from those of cortical sites that did not respond to electrical stimulation. Auditory response properties analyzed were best frequency and response latency.

We also obtained evidence that electrical stimulation of the dopaminergic ventral midbrain evoked excitatory and inhibitory responses in single units in auditory cortex. This was found when we analyzed 57 single units which were isolated from the 140 sites where electrically evoked responses were observed in the multiunit activity. Inspection of the PSTHs triggered on the onset of the electrical stimulus suggested weak electrically evoked responses in several single units with none being statistically significant. To quantitatively describe electrically evoked responses in single units nevertheless, we generated two population



PSTHs from the firing of the 57 single units. The first population consisted of the 42 single units that were recorded from sites where an excitatory electrically evoked multiunit response was detected (Fig. 6e). A Wilcoxon test (two-sided,  $p < 0.05$ ) revealed an excitatory electrical response lasting from 20 to 140 ms after stimulus onset. The second population consisted of the 15 single units where an inhibitory electrically evoked multiunit response

was detected (Fig. 6f). A Wilcoxon test revealed an inhibitory electrical response lasting from 70 to 200 ms after stimulus onset.

Electrically evoked multiunit responses are affected by the D1-receptor antagonist SCH23390

Like the EEPs, we found that multiunit responses to electrical stimulation of the dopaminergic ventral midbrain were under control of D1-receptors. Blocking them with the antagonist SCH23390 could attenuate or amplify such electrical responses in auditory cortex. These effects were seen both with intramuscular and intracortical injections.

Figure 7a shows a site with an excitatory response to electrical stimulation of the dopaminergic ventral midbrain (light blue curve). This response became smaller or even disappeared shortly after injection of the D1-receptor antagonist (red curve). The effect of the antagonist lasted for 30 min after which the excitatory response was recovered (dark blue curve). Note that the changes of the electrical response were accompanied by a temporary reduction of the spontaneous firing of the multiunit.

Figure 7b shows an example in which the D1-receptor antagonist had the opposite effect on the neural transmission from the dopaminergic ventral midbrain to auditory cortex. The neurons at this site usually did not respond to electrical stimulation (light blue curve). Within 5 min after injection, however, electrical stimulation was able to evoke an inhibitory response (according to our criterion) and this could be repeated during a period of 50 min (red curve), after which no more inhibitory responses could be evoked (dark blue curve). Note that also in this example the antagonist changed the spontaneous firing of the multiunit, however, it increased it. Presumably only this increase in spontaneous firing made it possible that the inhibitory action from the dopaminergic ventral midbrain was able to affect the (suprathreshold) firing.

The two types of effects of the antagonist SCH23390 on electrically evoked multiunit responses were seen at 39 sites in auditory cortex, including the two examples shown in Fig. 7, with no obvious differences between intramuscular and intracortical injections. This was found when we analyzed multiunit activity at 184 sites primarily in the granular layer of auditory cortex while electrical stimulation was applied at 47 sites in the dopaminergic ventral midbrain. Twenty sites in auditory cortex at which electrical responses were evoked under normal conditions lost their responses after injection of the antagonist. This was observed both for sites with excitatory responses (7) and for sites with inhibitory responses (13). The antagonist had no effect on six sites in auditory cortex at which electrical responses were evoked under normal conditions. At another 19 sites in auditory cortex, we observed that

electrical responses could temporarily be evoked after injection of the antagonist. Most of them were inhibitory responses (13), a smaller fraction were excitatory responses (6). No such emergence of responses was seen in 22 multiunits in auditory cortex at which we tested physiological saline instead of SCH23390. The time window during which the D1-receptor antagonist SCH23390 was effective was similar to that for EEPs, i.e., it was in the range of 5–60 min after drug injection. This is consistent with previous observation in primate prefrontal cortex (Sawaguchi and Goldman-Rakic 1994). At many sites, the change of an electrical response was accompanied by a change of the spontaneous firing, mostly an increase. These changes could also occur at sites that did not respond to electrical stimulation in any condition.

## Discussion

The current study on awake macaque monkeys shows for the first time that electrical stimulation of the dopaminergic ventral midbrain resulted in short-latency phasic activation of auditory cortex. Activations were reflected in local field potentials and spikes recorded in all cortical layers of auditory cortex and were also seen in the secondary somatosensory cortex and the superior temporal polysensory cortex. This shows that these cortices are under control of dopaminergic cell structures in the ventral midbrain. In the following, we discuss that these activations are most likely generated by non-dopaminergic transmitters, that dopamine modulates this transmission, and that they provide one source for the representation of non-auditory aspects of auditory tasks in the auditory cortex.

### Spatial spread of electrical stimulation

In this study, placement of stimulation electrodes was guided by a combination of stereotactic and physiological criteria. These included observing firing that is characteristic of dopaminergic neurons (e.g., Grace and Bunney 1983, 1984a, b) and finding neighboring brain nuclei with characteristic physiological properties, such as the red nucleus (Lovell et al. 2014). At selected locations, we verified that electrical stimulation excited dopaminergic neurons by demonstrating that the EEP in auditory cortex was modified by the D1-receptor antagonist SCH23390. These tests also revealed that stimulating different locations of the dopaminergic ventral midbrain elicited EEPs that were highly similar to one another. Stimulation of sites outside the dopaminergic ventral midbrain either elicited no EEP or an EEP of different shape. These could be elicited from auditory structures like medial geniculate body or from structures classically not considered part of

the auditory system. For example, Fig. 3a shows an EEP of a different shape that was elicited from the red nucleus and which we have considered to be indicative of a functional connection to the auditory cortex (Lovell et al. 2014). Thus, we concluded that the shape of the EEP can be used as an additional means for correct placement of an electrode in the dopaminergic ventral midbrain.

When we applied our criteria, we found EEPs with a shape that was specific for the dopaminergic ventral midbrain within a range extending about 9 mm in dorsolateral–medioventral direction. This matched very well with the published coordinates of the ventral tegmental area and substantia nigra. It is reasonable to assume that the stimulation parameters standardly used in the present study (100  $\mu$ A, monopolar, anodal first) excited neurons mainly within a radius of less than 1 mm (Ranck 1975; Histed et al. 2009). This estimation is supported by finding clear boundaries between different deep brain structures. For example, there was an abrupt change of the EEP shapes at 23.25 mm, when the stimulation electrode was moved from the red nucleus into the ventral tegmental area (see Fig. 3a). Thus, our stimulations were quite focal and in most cases, confined to one of the two dopaminergic nuclei. Within the two dopaminergic nuclei, the electrical stimulus likely excited dopaminergic, glutamatergic, and GABAergic neurons (and possibly also fibers of several brain stem nuclei that pass through the ventral tegmental area), with no obvious differences of EEPs between ventral tegmental area and substantia nigra. This was unexpected for us given that the two dopaminergic nuclei are generally considered to be part of distinct projection systems, namely the mesocortical and the nigrostriatal pathway (Oades and Halliday 1987). It is possible that this distinction is not as strict for auditory cortex because a recent study on rodents found that auditory cortex receives more projections from the substantia nigra than from the ventral tegmental area (Budinger et al. 2008). Because of the short latencies of the electrically evoked activations in auditory cortex and the conduction velocity of the mesocortical pathway (Deniau et al. 1980; Thierry et al. 1980), and because all cell types participate in the mesocortical projection to the prefrontal cortex (Thierry et al. 1973; Steffensen et al. 1998; Hur and Zaborszky 2005) we concluded that the earliest electrically evoked activations of auditory cortex are likely due to the monosynaptic connections from the dopaminergic ventral midbrain to auditory cortex. The effects found after injection of the D1-receptor antagonist (Fig. 2) argue against that electrically evoked responses arise from antidromic activation of cortical fibers projecting to the dopaminergic ventral midbrain or from activations of fibers of passage. This is consistent with more extended testing performed on the mesocortical system in rats (Lavin et al. 2005).

### Comparison of electrically evoked responses in different cortical areas

Our study is in good agreement with previous studies on prefrontal cortex that electrical stimulation of the ventral tegmental area and substantia nigra results in short-latency and short-lasting neuronal activations of cortex and that this is reflected in postsynaptic potentials (Bernardi et al. 1982; Ferron et al. 1984; Mercuri et al. 1985; Lavin et al. 2005), in extracellular field potentials (Lavin et al. 2005) and in neuronal firing (Pirot et al. 1992; Au Young et al. 1999; Pistis et al. 2001; Lavin et al. 2005). In the following, we argue that most of the differences of electrically evoked responses in prefrontal and auditory cortex reside in methodological and species differences and not in differences how the dopaminergic ventral midbrain affects neuronal activity in different cortical regions.

Latencies of electrically evoked responses were longer in sensory cortex than in prefrontal cortex. One reason for this is that our measurements were made in monkeys with larger brains and thus larger transmission times than those of rodents. Another and possibly more important reason is the effect of anesthesia, which reduces response latencies and which was used in all studies of prefrontal cortex, but not in the current study. For example, median minimum latency of acoustic responses in primary auditory cortex was 12 ms shorter in anesthetized animals than in awake animals (Ter-Mikaelian et al. 2007). Therefore, the anesthesia-induced reduction of response latencies could account for latency differences between prefrontal cortex and sensory cortex. It should also be noted that the stimulus artifact prohibited observation of latencies below 20 ms in our study.

The choice of stimulation parameters may explain why electrically evoked responses consisted of fewer waves in prefrontal cortex than in sensory cortex. For instance, Lavin and colleagues (Lavin et al. 2005) found that using a short pulse train instead of a single pulse, evoked potentials in prefrontal cortex with more than the maximally two components that have typically been reported in the prefrontal studies.

Similar to prefrontal cortex, stimulation of the dopaminergic ventral midbrain resulted in phasic increases and decreases of the neuronal firing in auditory cortex. These responses lasted for similar periods of time, with excitatory responses occurring earlier than inhibitory responses and every site (with 1 exception) exhibiting either an excitatory or an inhibitory response only. A difference, however, was that we found equal numbers of the two types of neuronal responses whereas in the prefrontal cortex, inhibitory responses prevailed. One reason for this may be that different cortical cell types show different electrical responses. Tseng et al. (2006) showed that pyramidal cells

responded with an inhibition after activating the ventral tegmental area with a small NMDA injection, whereas fast-spiking interneurons increased firing after such an injection. Because our study was based on multiunit activity, our data include both pyramidal cells and other cell types, such as cortical inhibitory interneurons. By contrast most of the studies on prefrontal cortex were likely biased toward pyramidal cells because these cells fire large action potentials that are more easily isolated in extracellular single unit recordings.

Our study also agrees with previous work on the mesocortical system that electrical responses in cortex are under dopaminergic control. For instance, we found that the D1-receptor antagonist SCH23390 modified the shape of EEPs and the strength of evoked firing in auditory cortex. This is consistent with the study of Lavin and colleagues (2005) who found that after local destruction of dopaminergic cells with 6-hydroxydopamine, stimulation of the ventral tegmental area failed to evoke postsynaptic potentials in the prefrontal cortex. This finding was confirmed for the electrically evoked depolarizations (but not for the subsequent hyperpolarizations) that were observed by optical imaging of neuronal activity with a voltage-sensitive dye (Watanabe et al. 2009). The cited studies also tested other transmitter systems and identified that the initial fast excitatory response was mediated by glutamate. Further tests suggested that this transmitter was probably coreleased by the dopaminergic terminals in cortex and not released from glutamatergic projection neurons in the ventral tegmental area (Lavin et al. 2005). Lavin et al. (2005) also found evidence that the following inhibitory potential was mediated by GABA.

Because of the large similarities of the electrically evoked responses in the auditory cortex, the somatosensory cortex, the superior temporal polysensory cortex (this study), and prefrontal cortex (e.g., Lavin et al. 2005; Watanabe et al. 2009), we consider that the electrically evoked responses in sensory cortex are also generated by glutamate that is coreleased from the dopaminergic terminals and by subsequent GABA-mediated inhibition. This is consistent with the conclusions of Seamans and Yang (2004) that the postsynaptic effects of dopamine are too slow to generate EEPs with a short-latency and a short duration. Nevertheless, one has to take into account that the density of dopaminergic fibers falls off from rostral to caudal parts of the cortex, thus, that the mesocortical pathway likely has a stronger effect on the prefrontal cortex than on the sensory cortex (Swanson 1982; Björklund and Lindvall 1984; Lewis et al. 1987; Berger et al. 1991; Durstewitz et al. 1999).

In conclusion, electrical stimulation in the dopaminergic ventral midbrain appears to similarly affect neuronal activity in different regions of the auditory cortex, the

somatosensory cortex, the superior temporal polysensory cortex, and the prefrontal cortex. Whether this also applies to other cortical regions is brought into question by an imaging study using voltage-sensitive dyes. It was reported that electrical stimulation in the ventral tegmental area evoked changes in optical signals only within an entire field of prefrontal cortex but spared adjoining primary motor cortex and more remote primary somatosensory cortex (Watanabe et al. 2009).

#### Layer-specific activation of auditory cortex by electrical stimulation

Our CSD analysis suggests that the volley of action potential evoked by electrical stimulation of the dopaminergic ventral midbrain initiates a stereotypic layer-specific activation sequence in auditory cortex. It is initially most pronounced in the infragranular layer and subsequently proceeds from the granular layer back to the infragranular and to the supragranular layer. Because the initial part of the EEP is most likely mediated by glutamate (see above), our results suggest that the density of the mesocortical glutamate (co)release sites is highest in the infragranular layer of auditory cortex. Although to our knowledge this question has not yet been addressed anatomically, it is interesting that this corresponds to reports that the density of dopaminergic terminals is highest in infragranular layers (Campbell et al. 1987; Lewis et al. 1987). The higher density of the dopaminergic terminals in the infragranular layers entails an increased probability for the occurrence of glutamate release sites.

To our surprise, the sequence of activations evoked by electrical stimulation of the dopaminergic ventral midbrain mirrored the sequence of activations in auditory cortex evoked by auditory stimulation. The delayed progression of the intracolumnar signal flow after electrical stimulation might simply reflect differences in the strength of stimulation. The similarities of the spatial cascades might be due to the recruitment of the same transmitter systems after auditory and electrical stimulation. They also suggest that the later electrically evoked activations in auditory cortex reflect a mixture of currents arising from intracolumnar and extracolumnar inputs (Happel et al. 2010, 2014) and from polysynaptic inputs from the dopaminergic ventral midbrain.

#### Functional implications

The current electrical stimulation study indicates that fluctuations of neuronal activity in the dopaminergic ventral midbrain are rapidly conveyed to auditory cortex and other parts of sensory cortex. Here they depolarize and sometimes also hyperpolarize neurons in all layers for up to

a few hundred milliseconds. In a substantial fraction of these neurons, the changes of membrane potentials are suprathreshold and even affect their firing. Thus, the mesocortical projection may contribute to the synchronization of neurons in the dopaminergic ventral midbrain with auditory, secondary somatosensory, or superior temporal polysensory cortex, as has been demonstrated for the prefrontal cortex (Gao et al. 2007; Fujisawa and Buzsáki 2011).

On a functional level our findings suggest that information carried by neurons in the dopaminergic ventral midbrain is rapidly conveyed to auditory cortex and other parts of sensory cortex. In the ventral midbrain, dopaminergic neurons have been implicated in encoding motivational value (seeking goals, evaluating outcomes, and value learning) or motivational salience (orienting, cognitive processing, and drive), thus providing an alerting signal (Bromberg-Martin et al. 2010; Schulz 2008). Glutamatergic neurons may also carry such information because selective activation of these cells promotes reward (Wang et al. 2013). These cells may also contribute to locomotor responses (Birgner et al. 2010; Hnasko et al. 2012). GABAergic neurons showed persistent activity during the interval between a reward-predicting odor and the subsequent reward (Cohen et al. 2012). Our findings also suggest that the projection from the dopaminergic ventral midbrain contributes to our previous observations of firing in auditory cortex that represents reward-related information, including reward expectancy errors (Brosch et al. 2011a). Current results are also compatible with the proposal by Seamans and Yang (2004) for the prefrontal cortex that the early activation by stimulating the dopaminergic ventral midbrain initiates the persistent activity states of cortical networks that allow for control of cognitive functions, such as holding information about auditory stimuli in a working memory buffer (Huang et al. 2012) or more generally to inform cortical networks when certain information should be represented (Brosch et al. 2011b). It should be noted that in addition to fast mesocortical information transmission by amino acid neurotransmitters, the dopaminergic ventral midbrain also affects auditory cortex on a slower timescale by the monoaminergic neurotransmitter dopamine that is released from terminals in this cortical structure and taken up by different dopamine receptor types and might serve different roles (Stark and Scheich 1997; Bao et al. 2001, 2003; Schicknick et al. 2008, 2012; Weis et al. 2012).

**Acknowledgments** The authors thank Dr. Jörg Stadler for MRI measurements and Drs. Eike Budinger, Nikolaos Aggelopoulos, and Daniel Zaldivar for valuable suggestions on the manuscript. The work was supported by the Deutsche Forschungsgemeinschaft (DFG, SFB 779), the federal state of Saxony-Anhalt and the European Regional Development Fund (ERDF 2007–2013) and the Russian Science Foundation (RSCF 14-28-00229).

**Conflict of interest** There are no conflicts of interest.

## References

- Amunts K, Morosan P, Hilbig H, Zilles K (2012) Auditory system: cyto-, myelo-, and receptor architecture of the auditory cortex. In: Mai JK, Paxinos G (eds) *The human nervous system*, 3rd edn. Elsevier Academic Press, San Diego, pp 1257–1287
- Arsenault JT, Nelissen K, Jarraya B, Vanduffel W (2013) Dopaminergic reward signals selectively decrease fMRI activity in primate visual cortex. *Neuron* 77(6):1174–1186
- Atzori M, Kanold PO, Pineda JC, Flores-Hernandez J, Paz RD (2005) Dopamine prevents muscarinic-induced decrease of glutamate release in the auditory cortex. *Neuroscience* 134(4):1153–1165
- Au-Young SM, Shen H, Yang CR (1999) Medial prefrontal cortical output neurons to the ventral tegmental area (VTA) and their responses to burst-patterned stimulation of the VTA: neuroanatomical and in vivo electrophysiological analyses. *Synapse* 34:245–255
- Bao S, Chan VT, Merzenich MM (2001) Cortical remodelling induced by activity of ventral tegmental dopamine neurons. *Nature* 412:79–83
- Bao S, Chan VT, Zhang LI, Merzenich MM (2003) Suppression of cortical representation through backward conditioning. *Proc Natl Acad Sci USA* 100:1405–1408
- Berger B, Gaspar P, Verney C (1991) Dopaminergic innervation of the cerebral cortex: unexpected differences between rodents and primates. *Trends Neurosci* 14(1):21–27
- Bernardi G, Cherubini E, Marciani MG, Mercuri N, Stanzione P (1982) Responses of intracellularly recorded cortical neurons to the iontophoretic application of dopamine. *Brain Res* 245:267–274
- Birgner C, Nordenankar K, Lundblad M, Mendez JA, Smith C, le Grevès M, Galter D, Olson L, Fredriksson A, Trudeau LE, Kullander K, Wallén-Mackenzie A (2010) VGLUT2 in dopamine neurons is required for psychostimulant-induced behavioral activation. *Proc Natl Acad Sci USA* 107(1):389–394
- Björklund A, Lindvall O (1984) Dopamine-containing systems in the CNS. In: Björklund A, Hökfelt T (eds) *Handbook of chemical neuroanatomy: classical transmitter in the rat*, vol 2. Elsevier/North Holland, Amsterdam, pp 55–122
- Bromberg-Martin ES, Matsumoto M, Hikosaka O (2010) Dopamine in motivational control: rewarding, aversive, and alerting. *Neuron* 68(5):815–834
- Brosch M, Schulz A, Scheich H (1999) Processing of sound sequences in macaque auditory cortex: response enhancement. *J Neurophysiol* 82(3):1542–1559
- Brosch M, Scheich H (2008) Tone-sequence analysis in the auditory cortex of awake macaques. *Exp Brain Res* 184(3):349–361
- Brosch M, Selezneva E, Scheich H (2011a) Representation of reward feedback in primate auditory cortex. *Front Syst Neurosci* 5:5
- Brosch M, Selezneva E, Scheich H (2011b) Formation of associations in auditory cortex by slow changes of tonic firing. *Hear Res* 271(1–2):66–73
- Budinger E, Laszcz A, Lison H, Scheich H, Ohl FW (2008) Non-sensory cortical and subcortical connections of the primary auditory cortex in Mongolian gerbils: bottom-up and top-down processing of neuronal information via field AI. *Brain Res* 1220:2–32
- Campbell MJ, Lewis DA, Foote SL, Morrison JH (1987) Distribution of choline acetyltransferase-, serotonin-, dopamine-beta-hydroxylase-, tyrosine hydroxylase-immunoreactive fibers in monkey primary auditory cortex. *J Comp Neurol* 261(2):209–220

- Carr DB, Sesack SR (2000) GABA-containing neurons in the rat ventral tegmental area project to the prefrontal cortex. *Synapse* 38(2):114–123
- Chiodo LA (1988) Dopamine-containing neurons in the mammalian central nervous system: electrophysiology and pharmacology. *Neurosci Biobehav Rev* 12(1):49–91
- Chudasama Y, Robbins TW (2004) Dopaminergic modulation of visual attention and working memory in the rodent prefrontal cortex. *Neuropsychopharmacology* 29(9):1628–1636
- Cohen JY, Haesler S, Vong L, Lowell BB, Uchida N (2012) Neuron-type-specific signals for reward and punishment in the ventral tegmental area. *Nature* 482(7383):85–88
- Delgado JM (1965) Sequential behavior induced repeatedly by stimulation of the red nucleus in free monkeys. *Science* 148(3675):1361–1363
- Deniau JM, Thierry AM, Feger J (1980) Electrophysiological identification of mesencephalic ventromedial tegmental (VMT) neurons projecting to the frontal cortex, septum and nucleus accumbens. *Brain Res* 189:315–326
- Diana M, Garcia-Munoz M, Richards J, Freed CR (1989) Electrophysiological analysis of dopamine cells from the substantia nigra pars compacta of circling rats. *Exp Brain Res* 74(3):625–630
- Durstewitz D, Kröner S, Güntürkün O (1999) The dopaminergic innervation of the avian telencephalon. *Prog Neurobiol* 59(2):161–195
- Ferron A, Thierry AM, Le Douarin C, Glowinski J (1984) Inhibitory influence of the mesocortical dopaminergic system on spontaneous activity or excitatory response induced from the thalamic mediodorsal nucleus in the rat medial prefrontal cortex. *Brain Res* 302(2):257–265
- Fields HL, Hjelmstad GO, Margolis EB, Nicola SM (2007) Ventral tegmental area neurons in learned appetitive behavior and positive reinforcement. *Annu Rev Neurosci* 30:289–316
- Freeman AS, Bunney BS (1987) Activity of A9 and A10 dopaminergic neurons in unrestrained rats: further characterization and effects of apomorphine and cholecystokinin. *Brain Res* 405(1):46–55
- Freeman AS, Meltzer LT, Bunney BS (1985) Firing properties of substantia nigra dopaminergic neurons in freely moving rats. *Life Sci* 36(20):1983–1994
- Fritz J, Mishkin M, Saunders RC (2005) In search of an auditory engram. *Proc Natl Acad Sci USA* 102(26):9359–9364
- Fujisawa S, Buzsáki G (2011) A 4 Hz oscillation adaptively synchronizes prefrontal, VTA, and hippocampal activities. *Neuron* 72(1):153–165
- Gao M, Liu CL, Yang S, Jin GZ, Bunney BS, Shi WX (2007) Functional coupling between the prefrontal cortex and dopamine neurons in the ventral tegmental area. *J Neurosci* 27:5414–5421
- Gaspar P, Stepniewska I, Kaas JH (1992) Topography and collateralization of the dopaminergic projections to motor and lateral prefrontal cortex in owl monkeys. *J Comp Neurol* 325(1):1–21
- Gibson AR, Houk JC, Kohlerman NJ (1985) Magnocellular red nucleus activity during different types of limb movement in the macaque monkey. *J Physiol* 358:527–549
- Gittelman JX, Perkel DJ, Portfors CV (2013) Dopamine modulates auditory responses in the inferior colliculus in a heterogeneous manner. *J Assoc Res Otolaryngol* 14(5):719–729
- Grace AA (1991) Regulation of spontaneous activity and oscillatory spike firing in rat midbrain dopamine neurons recorded in vitro. *Synapse* 7(3):221–234
- Grace AA, Bunney BS (1980) Nigral dopamine neurons: intracellular recording and identification with L-dopa injection and histofluorescence. *Science* 210(4470):654–656
- Grace AA, Bunney BS (1983) Intracellular and extracellular electrophysiology of nigral dopaminergic neurons—1. Identification and characterization. *Neuroscience* 10(2):301–315
- Grace AA, Bunney BS (1984a) The control of firing pattern in nigral dopamine neurons: burst firing. *J Neurosci* 4(11):2877–2890
- Grace AA, Bunney BS (1984b) The control of firing pattern in nigral dopamine neurons: single spike firing. *J Neurosci* 4(11):2866–2876
- Grace AA, Onn SP (1989) Morphology and electrophysiological properties of immunocytochemically identified rat dopamine neurons recorded in vitro. *J Neurosci* 9(10):3463–3481
- Guyenet PG, Aghajanian GK (1978) Antidromic identification of dopaminergic and other output neurons of the rat substantia nigra. *Brain Res* 150(1):69–84
- Happel MF, Jeschke M, Ohl FW (2010) Spectral integration in primary auditory cortex attributable to temporally precise convergence of thalamocortical and intracortical input. *J Neurosci* 30(33):11114–11127
- Happel MF, Deliano M, Handschuh J, Ohl FW (2014) Dopamine-modulated recurrent corticoefferent feedback in primary sensory cortex promotes detection of behaviorally relevant stimuli. *J Neurosci* 34(4):1234–1247
- Histed MH, Bonin V, Reid RC (2009) Direct activation of sparse, distributed populations of cortical neurons by electrical microstimulation. *Neuron* 63(4):508–522
- Hnasko TS, Hjelmstad GO, Fields HL, Edwards RH (2012) Ventral tegmental area glutamate neurons: electrophysiological properties and projections. *J Neurosci* 32(43):15076–15085
- Hosp JA, Pekanovic A, Rioult-Pedotti MS, Luft AR (2011) Dopaminergic projections from midbrain to primary motor cortex mediate motor skill learning. *J Neurosci* 31:2481–2487
- Houk JC, Gibson AR, Harvey CF, Kennedy PR, van Kan PL (1988) Activity of primate magnocellular red nucleus related to hand and finger movements. *Behav Brain Res* 28(1–2):201–206
- Huang Y, Zacharias N, König R, Brosch M, Heil P (2012) Physiological mechanisms of working memory in the auditory cortex of humans and nonhuman primates. 34th ARO Meeting Abstr 470:164
- Hur EE, Zaborszky L (2005) VGLUT2 afferents to the medial prefrontal and primary somatosensory cortices: a combined retrograde tracing in situ hybridization study. *J Comp Neurol* 483(3):351–373
- Irvine DR (1980) Acoustic input to neurons in feline red nucleus. *Brain Res* 200(1):169–173
- Jacob SN, Ott T, Nieder A (2013) Dopamine regulates two classes of primate prefrontal neurons that represent sensory signals. *J Neurosci* 33(34):13724–13734
- Jay TM, Glowinski J, Thierry AM (1995) Inhibition of hippocampoprefrontal cortex excitatory responses by the mesocortical DA system. *NeuroReport* 6(14):1845–1848
- Jervis BW, Nichols MJ, Johnson TE, Allen E, Hudson NR (1983) A fundamental investigation of the composition of auditory evoked potentials. *IEEE Trans Biomed Eng* 30(1):43–50
- Kajikawa Y, Schroeder CE (2011) How local is the local field potential? *Neuron* 72(5):847–858
- Kaur S, Rose HJ, Lazar R, Liang K, Metherate R (2005) Spectral integration in primary auditory cortex: laminar processing of afferent input, in vivo and in vitro. *Neuroscience* 134(3):1033–1045
- Kennedy PR, Gibson AR, Houk JC (1986) Functional and anatomic differentiation between parvocellular and magnocellular regions of red nucleus in the monkey. *Brain Res* 364(1):124–136
- Kiyatkin EA (1988) Morphine-induced modification of the functional properties of ventral tegmental area neurons in conscious rat. *Int J Neurosci* 41(1–2):57–70
- Kiyatkin EA, Zhukov VN (1988) Impulse activity of mesencephalic neurons on nociceptive stimulation in awake rats. *Neurosci Behav Physiol* 18(5):393–400

- Kudoh M, Shibuki K (2006) Sound sequence discrimination learning motivated by reward requires dopaminergic D2 receptor activation in the rat auditory cortex. *Learn Mem* 13:690–698
- Larsen KD, Yumiya H (1980) The red nucleus of the monkey. Topographic localization of somatosensory input and motor output. *Exp Brain Res* 40(4):393–404
- Lavin A, Nogueira L, Lapish CC, Wightman RM, Phillips PE, Seamans JK (2005) Mesocortical dopamine neurons operate in distinct temporal domains using multimodal signaling. *J Neurosci* 25(20):5013–5023
- Lewis DA, Campbell MJ, Foote SL, Goldstein M, Morrison JH (1987) The distribution of tyrosine hydroxylase-immunoreactive fibers in primate neocortex is widespread but regionally specific. *J Neurosci* 7(1):279–290
- Lidow MS, Goldman-Rakic PS, Gallager DW, Rakic P (1991) Distribution of dopaminergic receptors in the primate cerebral cortex: quantitative autoradiographic analysis using [<sup>3</sup>H]raclopride, [<sup>3</sup>H]spiperone and [<sup>3</sup>H]SCH23390. *Neuroscience* 40(3):657–671
- Lovell JM, Mylius J, Scheich H, Brosch M (2014) Hearing in action; auditory properties of neurones in the red nucleus of alert primates. *Front Neurosci* 8:105
- Mantz J, Milla C, Glowinski J, Thierry AM (1988) Differential effects of ascending neurons containing dopamine and noradrenaline in the control of spontaneous activity and of evoked responses in the rat prefrontal cortex. *Neuroscience* 27(2):517–526
- Margolis EB, Lock H, Hjelmstad GO, Fields HL (2006) The ventral tegmental area revisited: is there an electrophysiological marker for dopaminergic neurons? *J Physiol* 577(Pt 3):907–924
- Martin RF, Bowden DM (1996) A stereotaxic template atlas of the macaque brain for digital imaging and quantitative neuroanatomy. *Neuroimage* 4(2):119–150
- Massion J, Albe-Fessard D (1963) Duality of afferent sensory tracts controlling the activity of the red nucleus. *Electroencephalogr Clin Neurophysiol* 15:435–454
- Matsumura M, Sawaguchi T, Kubota K (1990) Modulation of neuronal activities by iontophoretically applied catecholamines and acetylcholine in the primate motor cortex during a visual reaction-time task. *Neurosci Res* 8(2):138–145
- Mercuri N, Calabresi P, Stanzione P, Bernardi G (1985) Electrical stimulation of mesencephalic cell groups (A9–A10) produces monosynaptic excitatory potentials in rat frontal cortex. *Brain Res* 338:192–195
- Mitzdorf U (1985) Current source-density method and application in cat cerebral cortex: investigation of evoked potentials and EEG phenomena. *Physiol Rev* 65(1):37–100
- Müller-Preuss P, Mitzdorf U (1984) Functional anatomy of the inferior colliculus and the auditory cortex: current source density analyses of click-evoked potentials. *Hear Res* 16(2):133–142
- Nicholson C, Freeman JA (1975) Theory of current source-density analysis and determination of conductivity tensor for anuran cerebellum. *J Neurophysiol* 38(2):356–368
- Oades RD, Halliday GM (1987) Ventral tegmental (A10) system: neurobiology. 1. Anatomy and connectivity. *Brain Res* 434(2):117–165
- Pirot S, Godbout R, Mantz J, Tassin JP, Glowinski J, Thierry AM (1992) Inhibitory effects of ventral tegmental area stimulation on the activity of prefrontal cortical neurons: evidence for the involvement of both dopaminergic and GABAergic components. *Neuroscience* 49:857–865
- Pistis M, Porcu G, Melis M, Diana M, Gessa GL (2001) Effects of cannabinoids on prefrontal neuronal responses to ventral tegmental area stimulation. *Eur J Neurosci* 14(1):96–102
- Ranck JB Jr (1975) Which elements are excited in electrical stimulation of mammalian central nervous system: a review. *Brain Res* 98(3):417–440
- Sawaguchi T, Goldman-Rakic PS (1991) D1 dopamine receptors in prefrontal cortex: involvement in working memory. *Science* 251(4996):947–950
- Sawaguchi T, Goldman-Rakic PS (1994) The role of D1-dopamine receptor in working memory: local injections of dopamine antagonists into the prefrontal cortex of rhesus monkeys performing an oculomotor delayed-response task. *J Neurophysiol* 71:515–528
- Sawaguchi T, Matsumura M (1985) Laminar distributions of neurons sensitive to acetylcholine, noradrenaline and dopamine in the dorsolateral prefrontal cortex of the monkey. *Neurosci Res* 2(4):255–273
- Sawaguchi T, Matsumura M, Kubota K (1986) Catecholamine sensitivities of motor cortical neurons of the monkey. *Neurosci Lett* 66(2):135–140
- Sayers BM, Beagley HA, Henshall WR (1974) The mechanism of auditory evoked EEG responses. *Nature* 247(5441):481–483
- Scheibner T, Törk I (1987) Ventromedial mesencephalic tegmental (VMT) projections to ten functionally different cortical areas in the cat: topography and quantitative analysis. *J Comp Neurol* 259(2):247–265
- Schicknick H, Schott BH, Budinger E, Smalla KH, Riedel A, Seidenbecher CI, Scheich H, Gundelfinger ED, Tischmeyer W (2008) Dopaminergic modulation of auditory cortex-dependent memory consolidation through mTOR. *Cereb Cortex* 18:2646–2658
- Schicknick H, Reichenbach N, Smalla KH, Scheich H, Gundelfinger ED, Tischmeyer W (2012) Dopamine modulates memory consolidation of discrimination learning in the auditory cortex. *Eur J Neurosci* 35(763–74):2012
- Schultz W (1998) Predictive reward signal of dopamine neurons. *J Neurophysiol* 80:1–27
- Schultz W, Dayan P, Montague PR (1997) A neural substrate for prediction and reward. *Science* 275:1593–1599
- Schultz W, Preusschoff K, Camerer C, Hsu M, Fiorillo CD, Tobler PN, Bossaerts P (2008) Explicit neural signals reflecting reward uncertainty. *Philos Trans R Soc Lond B Biol Sci* 363(1511):3801–3811
- Seamans JK, Yang CR (2004) The principal features and mechanisms of dopamine modulation in the prefrontal cortex. *Prog Neurobiol* 74:1–58
- Smith Y, Wichmann T, DeLong MR (2013) Corticostriatal and mesocortical dopamine systems: do species differences matter? *Nat Rev Neurosci* 15(1):63
- Stark H, Scheich H (1997) Dopaminergic and serotonergic neurotransmission systems are differentially involved in auditory cortex learning: a long-term microdialysis study of metabolites. *J Neurochem* 68:691–697
- Steffensen SC, Svingos AL, Pickel VM, Henriksen SJ (1998) Electrophysiological characterization of GABAergic neurons in the ventral tegmental area. *J Neurosci* 18(19):8003–8015
- Steinschneider M, Tenke CE, Schroeder CE, Javitt DC, Simpson GV, Arezzo JC, Vaughan HG Jr (1992) Cellular generators of the cortical auditory evoked potential initial component. *Electroencephalogr Clin Neurophysiol* 84(2):196–200
- Steinschneider M, Reser DH, Fishman YI, Schroeder CE, Arezzo JC (1998) Click train encoding in primary auditory cortex of the awake monkey: evidence for two mechanisms subserving pitch perception. *J Acoust Soc Am* 104(5):2935–2955
- Supèr H, Roelfsema PR (2005) Chronic multiunit recordings in behaving animals: advantages and limitations. *Prog Brain Res* 147:263–282
- Swanson LW (1982) The projections of the ventral tegmental area and adjacent regions: a combined fluorescent retrograde tracer and immunofluorescence study in the rat. *Brain Res Bull* 9(1–6):321–353

- Szabo J, Cowan WM (1984) A stereotaxic atlas of the brain of the cynomolgus monkey (*Macaca fascicularis*). *J Comp Neurol* 222(2):265–300
- Ter-Mikaelian M, Sanes DH, Semple MN (2007) Transformation of temporal properties between auditory midbrain and cortex in the awake Mongolian gerbil. *J Neurosci* 27(23):6091–6102
- Thierry AM, Blanc G, Sobel A, Stinus L, Golwinski J (1973) Dopaminergic terminals in the rat cortex. *Science* 182(4111):499–501
- Thierry AM, Deniau JM, Herve D, Chevalier G (1980) Electrophysiological evidence for non-dopaminergic mesocortical and mesolimbic neurons in the rat. *Brain Res* 201(1):210–214
- Thierry AM, Godbout R, Mantz J, Pirot S, Glowinski J (1992) Differential influence of dopaminergic and noradrenergic afferents on their target cells in the rat prefrontal cortex. *Clin Neuropharmacol* 15 Suppl 1 Pt A:139–140
- Tseng KY, Mallet N, Toreson KL, Le Moine C, Gonon F, O'Donnell P (2006) Excitatory response of prefrontal cortical fast-spiking interneurons to ventral tegmental area stimulation in vivo. *Synapse* 59(7):412–417
- Wang HL, Qi J, Morales M (2013) Activation of ventral tegmental area glutamate neurons is rewarding. *SfN Abstr* 389:05
- Watanabe Y, Kajiwara R, Takashima I (2009) Optical imaging of rat prefrontal neuronal activity evoked by stimulation of the ventral tegmental area. *NeuroReport* 20:875–880
- Weis T, Puschmann S, Brechmann A, Thiel CM (2012) Effects of L-dopa during auditory instrumental learning in humans. *PLoS ONE* 7(12):e52504
- Williams SM, Goldman-Rakic PS (1998) Widespread origin of the primate mesofrontal dopamine system. *Cereb Cortex* 8:321–345
- Yamaguchi T, Wang HL, Li X, Ng TH, Morales M (2011) Mesocorticolimbic glutamatergic pathway. *J Neurosci* 31(23):8476–8490
- Zilles K, Palomero-Gallagher N, Grefkes C, Scheperjans F, Boy C, Amunts K, Schleicher A (2002) Architectonics of the human cerebral cortex and transmitter receptor fingerprints: reconciling functional neuroanatomy and neurochemistry. *Eur Neuropsychopharmacol* 12(6):587–599